UNIVERSITY OF TORINO
DEPARTMENT OF MEDICAL SCIENCES
DOCTORAL PROGRAMME IN MEDICAL PHYSIOPATHOLOGY – XXXIV CYCLE

THESIS

CHARACTERIZATION OF CIRCULATING EXTRACELLULAR VESICLE SURFACE ANTIGENS IN PATIENTS WITH PRIMARY ALDOSTERONISM

CANDIDATE: Dr. Jacopo BURRELLO

TUTOR: Prof. Paolo MULATERO

COORDINATOR: Prof. Franco VEGLIO

ACADEMIC YEARS: 2018-2021

MED/09

LIST of CONTENTS

LIST of TABLES & FIGURES

1. BACKGROUND

Primary aldosteronism (PA) is a frequent cause of endocrine hypertension affecting 6% of all hypertensive patients *[Monticone S, J Am Coll Cardiol 2017]*. PA is due to an inappropriate secretion of aldosterone by the adrenal glands and may result from either aldosterone producing adenoma (APA) or bilateral hyperaldosteronism (BiPA), which are treated by unilateral adrenalectomy or require life-long medical treatment with a mineralocorticoid receptor antagonist (MRA), respectively *[Funder JW J Clin Endocrinol Metab 2016]*.

A growing body of evidence supports the role of aldosterone as mediator of vascular remodelling, an active process resulting from collagen deposition in the extracellular matrix, hypertrophy of smooth muscle cells, and fibrosis of small resistance arteries *[Rizzoni D, J Clin Endocrinol Metab 2006]*.
At the vascular level, aldosterone induces endothelial dysfunction by inhibiting nitric oxide (NO) release and impairing endothelium-dependent vasodilation, which results in the loss of vascular reactivity and increased arterial stiffness *[Ikeda U, Eur J Pharmacol 1995; Farquharson CA, Clin Sci 2002; Bernini G, J Hypertens 2008]*. Moreover, aldosterone-related vascular inflammation (with perivascular leukocyte infiltration and arterial wall inflammation) was observed in both murine models and patients with PA *[Rocha R, Am J Physiol Heart Circ Physiol 2002; Van der Heijden CDCC, J Clin Endocrinol Metab 2020]*.
The crosstalk between endothelium, vascular structures and inflammatory cells leads to accelerated atherogenesis and a pro-thrombotic environment in PA *[Chen ZW, Int J Mol Sci 2019]*, which may contribute to their increased risk of cardiovascular events compared to patients with essential hypertension (EH) *[Monticone S, Lancet Diabetes Endocrinol 2018]*.

However, the molecular machinery that regulates these complex interactions remains largely unknown. In this context, the characterization of circulating extracellular vesicles (EVs) may help to unravel the mechanisms underlying

endothelial dysfunction, vascular inflammation, and remodelling in PA. EVs are bilayer-membrane nanoparticles (NPs) released by all cell types, carrying proteins, lipids, and nucleic acids, which reflect the activation state of parental cells *[Yanez-Mo M, J Extracell Vesicles 2015]*. In particular, endothelial injury, vascular damage, pro-thrombotic cascade and the activation of an inflammatory response affect the composition of circulating EV, resulting in a specific molecular signature *[Burrello J, J Cell Mol Med 2020; Castellani C, J Heart Lung Transplant 2020]*. Nevertheless, EVs may represent not only biomarkers, but also active effectors of endothelial dysfunction, potentially able to influence the development of organ damage in patients with PA *[Chen ZW, Int J Mol Sci 2019; Burrello J, Hypertension 2019]*.

Our previous research indicates that circulating EVs from patients affected by PA display a different mRNA cargo compared with patients affected by EH and that PA-derived EVs promote apoptosis and inhibit angiogenesis in vitro *[Burrello J, Hypertension 2019]*.

Briefly, serum EVs were isolated from 12 patients with PA and 12 with EH, matched by sex, age, and blood pressure. EVs concentration was 2.2-fold higher in patients with PA and a significant correlation between EV number and serum aldosterone and potassium levels was identified. Flow cytometric analysis demonstrated that patients with PA displayed a higher number of leukocyte- and endothelial-derived EVs compared to patients with EH.

Through EV mRNA profiling, 16 up-regulated and 4 down-regulated genes in patients with PA. Microarray platform was then validated by quantative real-time polymerase chain reaction on 4 genes (*CASP1*, *EDN1*, *F2R*, and *HMOX1*) involved in apoptosis, inflammation, and endothelial dysfunction. Moreover, after unilateral adrenalectomy, EVs number and expression of *CASP1* and *EDN1* significantly decreased in patients with PA.

Finally, the incubation of human endothelial cells with PA-derived EVs reduced angiogenesis and induced apoptosis in vitro.

This was the first study which characterized serum-derived EVs in patients with PA, providing evidence of a functional effect of PA-derived EVs on endothelial cells in vitro. Hence, we hypothesized that circulating EVs might not only represent a marker of endothelial damage but also contribute themselves to vascular dysfunction in PA, suggesting their involvement in the development of endothelial dysfunction and accelerated organ damage displayed by these patients.

Therefore, we designed a second study to expand and confirm our findings on a larger cohort. We decided to perform a systematic evaluation of EV membrane proteins by a multiplex flow cytometric assay. Supervised learning algorithms and bioinformatic analysis applied to the immuno-profiling of antigens on EV surface, allowed us to discriminate patients with PA from EH, and to identify intracellular targets and molecular pathways potentially influenced by circulating EVs.

2. EXPERIMENTAL STUDY

2.1 *Aim of the Study*

The aim of the present study was to characterize circulating EV surface antigen profile in patients with PA, through an innovative flow cytometric multiplex bead-based platform, that evaluates the expression of a comprehensive panel of 37 membrane antigens expressed on the EV surface *[Koliha N, J Extracell Vesicles 2016; Wiklander OPB, Front Immunol 2018]*. Supervised machine learning algorithms were then used to combine the expression level of EV surface antigens in a specific signature to discriminate patients with PA from controls.

A bioinformatic network analysis of protein-protein interactors was performed to highlight potential molecular targets and biological pathways, that could be influenced by EV surface antigens differentially expressed in patients with PA compared to patients with EH. Finally, human endothelial cells were used as an in vitro model to explore the impact of EVs treatment on some of these targets, selected on the basis of their functional role.

2.2 *Methods*

Patients with PA, EH and normotensive (NT) controls were enrolled at the Hypertension Unit of the University of Torino, Italy. The study was approved by local ethical committee, and all patients gave fully informed written consent in accordance with the declaration of Helsinki.

Analytical factors for EV isolation, characterization and functional analysis complied with MISEV (Minimal Information for Studies of Extracellular Vesicles) indications *[Théry C, J Extracell Vesicles 2018]* by the International Society for Extracellular Vesicles (ISEV).

2.2.1 Patients and Blood Sampling

Diagnosis of PA was made according to the Endocrine Society (ES) and European Society of Hypertension (ESH) recommendations *[Funder JW, J Cli Endocrinol Metab 2016; Mulatero P, J Hypertens 2020; Mulatero P, J Hypertens 2020]*. The

cut-offs for a positive screening test were an aldosterone-to-renin ratio (ARR) greater than 30 ng/dL/ng*mL-1*h-1, together with and aldosterone concentration > 10 ng/dL. Patients with a positive screening test underwent confirmatory testing by intravenous saline loading test, or captopril challenge. Patients with confirmed PA underwent subtype differentiation through computed tomography scanning and adrenal venous sampling (AVS). Of the 20 patients with an aldosterone producing adenoma, 13 underwent unilateral adrenalectomy and were re-evaluated 6-12 months after surgery (APA-post). Of the 12 patients with bilateral PA (BiPA), 7 were re-evaluated after at least 6 months of medical treatment with mineralocorticoid receptor antagonists (BiPA-post). Samples for EV isolation and characterization were collected in the morning in fasting conditions just before AVS for patients with diagnosis of PA, or at screening for secondary forms of hypertension, for patients with EH. When antihypertensive medications could not be withdrawn, patients were treated calcium channel blockers or α-blockers. Common forms of secondary hypertension were excluded for patients with EH. Normotensive (NT) healthy volunteers were used as control.

2.2.2 Sample Handling and EV characterization

After peripheral venous blood sampling, blood underwent serial centrifugation cycles to separate serum and eliminate cellular debris and larger vesicles (see below). A commercially available assay (MACSPlex human Exosome Kit, Miltenyi; Bergisch Gladbach, Germany) was used to evaluate levels of expression of a standardized panel of EV surface antigens, including main markers from different blood cell types carried by circulating EVs *[Koliha N, J Extracell Vesicles 2016; Wiklander OPB, Front Immunol 2018]*. After bead-based immunocapture, EVs were then incubated with a detection buffer (fluorescently labeled antibodies for CD9/CD63/CD81) and analyzed by MACSQuant-Analyzer-10 flow cytometer (Miltenyi), according to a validated protocol *[Burrello J, J Cell Mol Med 2020]*. Beside bead-based flow cytometry, NPs were visualized by nanoparticle tracking analysis (NTA), and the presence of EV specific markers (TSG101, Syntenin-1, and CD81) and contaminants (GRP94 and

Apolipoprotein A1) was assessed by western blotting on protein lysate after EV immuno-capture. The term "nanoparticle(s)" is used instead of "extracellular vesicle(s)" when we referred to NTA. For the in vitro analysis, EVs were isolated by ultracentrifugation from aliquots of serum from selected patients for each subgroup, and characterized by transmission electron microscopy (TEM), western blot, flow cytometry and NTA (see below).

2.2.2.1 Sample handling

Peripheral venous blood samples were collected in 7 mL heparin-free tubes from patients in fasting conditions. Blood was centrifuged at 1,600 g for 15 minutes at 4°C to separate serum. Serum was centrifuged 3,000 g for 20 minutes, 10,000 g for 15 minutes, and 20,000 g for 30 minutes to remove intact cells, cellular debris, and larger EVs. After centrifugation, serum was stored at -80 °C, and never thawed prior to analysis.

2.2.2.2 EV isolation

Prior to multiplex bead-based flow cytometric analysis, EV were isolated by beads immuno-capture from 45 uL of serum, as described in Burrello et al. (see also paragraph 4.2.2.5).

For in vitro analysis, EVs were isolated by ultracentrifugation (100,000 g for 2 hours at 4 °C; Beckman Coulter Optima L-90K; Beckman Coulter, Fullerton, CA, USA). The pellet was resuspended in 100 uL of Phosphate Buffered Saline (PBS) solution. EVs were isolated from 3 mL serum aliquots; samples from 5 patients with a diagnosis of aldosterone producing adenoma (APA) and 5 with essential hypertension were pooled together, respectively.

2.2.2.3 Nanoparticle Tracking Analysis

Serum EVs were quantified by nanoparticle tracking analysis (NTA) using NanoSight LM10 (Malvern Instruments, United Kingdom) equipped with a 405 nm laser and Nanoparticle Tracking Analysis NTA 2.3 analytic software; 1 µL of serum was diluted 1:1000 in 999 µL NaCl 0.9% sterile solution and exposed to a

laser light source. A camera recorded Brownian movement of EVs and size and number of EVs per mL were calculated by Stokes-Einstein equation. Three videos of 60 s were recorded for each analysis. EV concentration is expressed as number of particles per 1 mL of serum.

2.2.2.4 Western Blot Analysis on EVs

Western Blot analysis was performed on protein lysate either after ultracentrifugation or after EV immuno-capture. For immunocapture, 60 uL of serum were incubated overnight on an orbital shaker (800 rpm at 10°C) with 10 uL of MACSPlex capture beads (MACSPlex human Exosome Kit, Miltenyi Biotec; Bergisch Gladbach, Germany) and 60 uL of saline buffer. Unbounded fraction was discarded, and samples were lysed in RIPA buffer. After ultracentrifugation, EV pellet was resuspended in RIPA buffer supplemented with 1% Protease Inhibitor Cocktail (Sigma Aldrich, St. Louis, MO, USA).

For both preparations (immuno-capture and ultracentrifugation), 15 ug of total proteins were separated on SDS Page 4-12% gel (BioRad) and transferred onto PVDF membrane. Membranes were incubated overnight at 4°C under gentle agitation with primary antibodies diluted in OBB-T. Membranes were then incubated with IR Dye® 680RD or 800CW goat anti-mouse or goat anti-rabbit secondary Ab (LI-COR Biosciences; 1:15000 dilution in OBB-T) at RT for 2 h. The infrared signal was detected by Odyssey CLx Detection System (LI-COR Biosciences). Blots of three representative samples were incubated with the following primary antibodies: rabbit monoclonal anti-TSG101 (Abcam #12501, 1:1000), mouse monoclonal anti-GRP94 (Abcam #108606, 1:500), rabbit polyclonal anti-Syntenin-1 (Abcam #19903, 1:1000), rabbit monoclonal anti-CD81 (Abcam #109201, 1:500), and rabbit monoclonal anti-Apolipoprotein A1 (Invitrogen #701239, 1:500).

2.2.2.5 Multiplex bead-based Flow Cytometry

Flow cytometry analysis was performed using MACSPlex human Exosome Kit (Miltenyi Biotec; Bergisch Gladbach, Germany), according to a previously

validated protocol (**Figure 1**) *[Burrello J, J Cell Mol Med 2020]*. Median fluorescence intensity (MFI) was measured by MACSQuant Analyzer 10 flow cytometer (Miltenyi Biotec; Bergisch Gladbach, Germany). The analysis is based on a multiplex platform which allows the simultaneous evaluation of 37 different EV surface antigens.

EVs are captured by polystyrene beads (MACSPlex Exosome Capture Beads), labelled with different amounts of 2 dyes (phycoerythrin [PE] and fluorescein isothiocyanate [FITC]), to generate 37 different bead-subsets discriminable by flow cytometry. Each bead subset is coated with a different antibody against a specific EV surface antigen. After incubation of beads and samples, captured EVs are detected by allophycocyanin [APC]-conjugated anti-CD9, anti-CD63, and anti-CD81 antibodies. Triggers for side scatter (SSC) and forward scatter (FSC) were set to confine the measurement on capture beads. FITC and PE voltage were optimized to discriminate the 37 bead subsets; single bead subsets were each gated to measure APC median fluorescence signal intensity (MFI).

Samples were processed as follow; 45 uL of serum (containing a number of particles per mL ranging between 1.0e9 e 5.0e10) were diluted to a final volume of 120 uL with MACSPlex buffer (MPB) and incubated overnight with 15 uL MACSPlex Exosome Capture Beads on an orbital shaker (800 rpm at 10°C) protected from light. MPB was used as blank control. After incubation, 1 mL of MPB was added to each tube and tubes were centrifuged 3.000 g for 10 minutes at 10°C to wash beads. After careful aspiration of 1 mL of supernatant, 15 uL of MACSPlex Exosome Detection Reagent (5 uL for each APC-conjugated anti-CD9, anti-CD63, and anti-CD8 antibody) were added and incubated for 1 hour on an orbital shaker (450 rpm at 10°C) protected from light. After another washing step, samples were analyzed by the instrument, resulting in approximately 10.000-15.000 single bead events being recorded for each sample. APC-MFI for each bead subset was corrected by subtracting the fluorescence value of blank control and then normalized by the mean MFI of CD9, CD63, and CD81. MFI was analyzed and reported throughout the manuscript for each EV surface antigen after normalization for blank control and mean MFI for CD9/CD63/CD81.

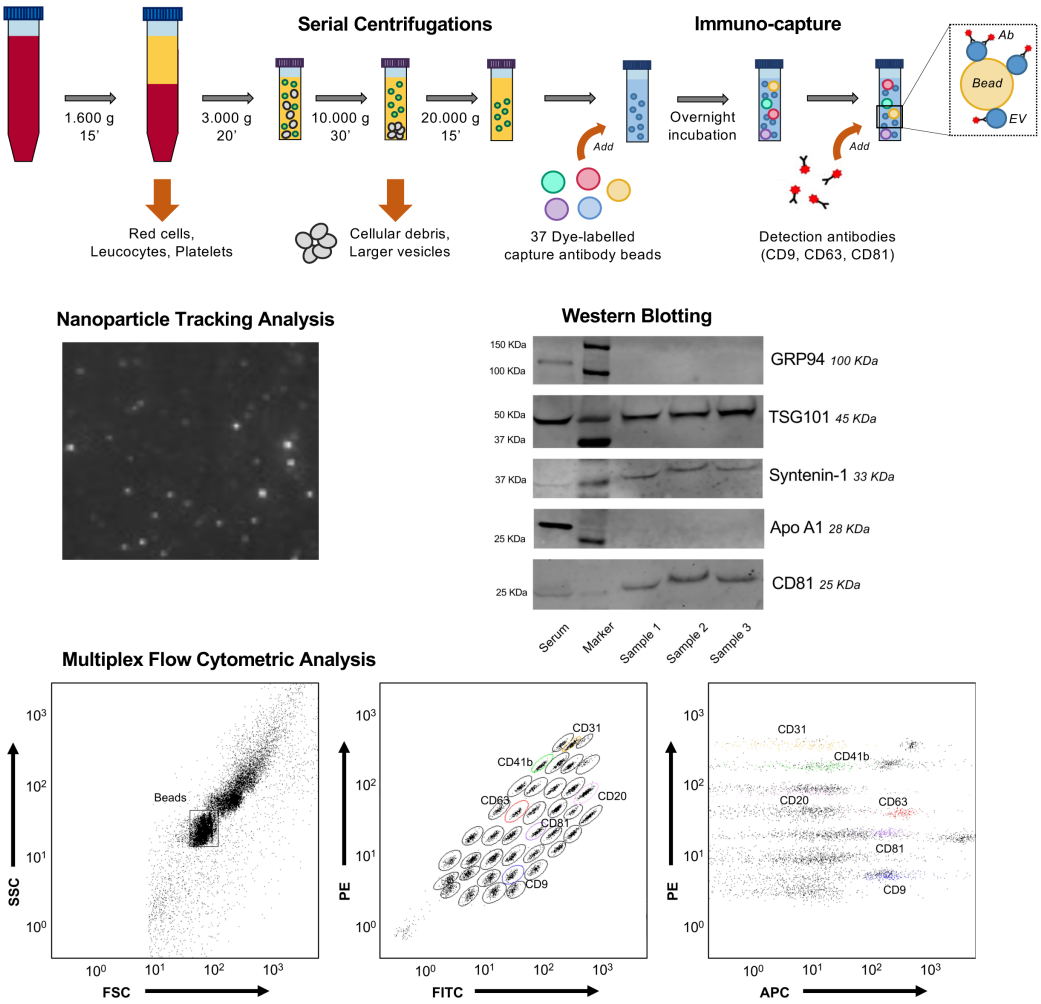

Figure 1. Study design and EV characterization *- Patient samples underwent serial centrifugation cycles to eliminate cells, cellular debris and larger vesicles. Extracellular vesicles (EVs) were isolated by beads immuno-capture (see methods) and characterized by nanoparticle tracking analysis (NTA; size and diameter), western blotting for TSG101, Syntenin-1 and CD81 (specific EV markers) and potential contaminants (GRP94 and ApoA1), and flow cytometric analysis, using a multiplex standardized assay for the evaluation of EV surface antigens.*

2.2.2.6 High-resolution Flow Cytometry

EVs isolated by ultracentrifugation were characterized by high-resolution flow cytometry (CytoFlex; Beckman Coulter). Approximately 5×10^{10} vesicles in 30 µL were incubated for 30 minutes at 4°C with the following antibodies: anti-CD9 (PE; Miltenyi Biotec, #130-103-955), anti-CD63 (FITC; Miltenyi Biotec, #130-100-160), anti-CD81 (PE; Miltenyi Biotec, #130-118-342), anti-CD3 (FITC; Miltenyi Biotec, #130-080-401), anti-CD20 (FITC; BD Biosciences, #23-5149-

00), anti-CD25 (PE; Invitrogen, #MHCD2504), anti-CD31 (PE; Miltenyi Biotec, #130-092-653), anti-CD45 (FITC; BD Biosciences, #555482). Final volume was increased to 100 µL with PBS.

Samples were acquired at low flow rate, using CytoFlex from Beckman Coulter. Instrument calibration and gating strategy were fulfilled according to manufacturer's instructions, using Cytoflex Daily QC Fluorospheres, followed by Megamix-Plus FSC reagent and Flow Count beads (0.1, 0.3, 0.5, and 0.9 µm; Biocytex; Diagnostica Stago).

Buffer alone with antibodies was analyzed to eliminate background noise during post-acquisition analysis. Disrupted EVs (high frequency sonication for 60 seconds) were used as negative control. Post-acquisition analysis was performed using CytExpert analysis software (Beckman Coulter).

2.2.2.7 Transmission Electron Microscopy

After isolation by ultracentrifugation, EVs were visualized by transmission electron microscopy; samples were loaded on 200 mesh nickel Formvar carbon-coated grids (Electron Microscopy Science, Hatfield, PA, USA) for 20 min, and then fixed with glutaraldehyde 2.5%, containing sucrose 2%. After washing steps, EVs were negatively stained with NanoVan (Nanoprobes, Yaphank, NY, USA) and observed by JEM-1010 electron microscope (Jeol, Tokyo, Japan).

2.2.3 In vitro analysis

Human microvascular endothelial cells (HMEC) were plated (30.000 cells/well) and starved using serum-free medium overnight. Then, the medium was changed, and cells were stimulated with EVs using a of dose 50.000 (EH patient derived EVs, or PA-EVs) or 165.000 EV/cells (APA patients derived EVs, or PA-EVs), reflecting the difference in EV concentration observed in our cohort between PA and EH patients. Non treated cells, cells treated with supernatant after ultracentrifugation, and cells treated with supernatant after bead-based immunocapture, were used as negative controls. EV preparation for the in vitro study was characterized by NTA, transmission electron microscopy (TEM),

western blot and high-resolution flow cytometry (as desctibed above).

After 24 hours of treatment, RNA was extracted using miRNeasy mini kit (Qiagen, Hilden, Germany) according to manufacturer's protocol. For each condition, 250 ng of RNA were reverse-transcripted using High-capacity cDNA Reverse Transcription Kit (Applied Biosystems, Thermo Fisher Scientific, Waltham, Massachusetts, USA).

Quantitative real-time polymerase chain reaction (qRT-PCR) analysis was performed using specific TaqMan assay for AKT1 (RAC-alpha serine/threonine-protein kinase; #Hs00178289-m1, Thermo Fisher Scientific), CALR (Calreticulin; #Hs00189032-m1, Thermo Fisher Scientific), CSNK2A1 (Casein kinase II subunit alpha; #Hs00751002-s1, Thermo Fisher Scientific), FN1 (Fibronectin; #Hs01549976-m1, Thermo Fisher Scientific), and PIK3R1 (Phosphatidylinositol 3-kinase regulatory subunit alpha; #s00933163-m1, Thermo Fisher Scientific). All primers (except the assay for CSNK2A1) were intro-spanning. For CSNK2A1, qRT-PCR was repeated after reverse-transcription with or without the use of reverse transcriptase to confirm absence of signal from genomic DNA (data not shown). Targets were selected among genes predicted as relevant hubs or bottlenecks by bioinformatic analysis (see below), considering their potential role in the regulation of renin-angiotensin-aldosterone system, aldosterone-mediated organ damage, and renal handling of sodium. Assays were performed using ABI 7,500 Fast Real-Time PCR System (Applied Biosystems), according to manufacturer's instructions. Each sample was run in duplicate. Gene expression levels were analyzed with the 2-ΔΔCT relative quantification method, using GAPDH (Glyceraldehyde 3-phosphate dehydrogenase), as endogenous control (#Hs02786624-g1, Thermo Fisher Scientific).

qRT-PCR was repeated for the same genes on cDNA from HMEC stimulated with EVs after treatment with glycine acid to remove EV membrane associated proteins. Briefly, EVs were incubated with 100 mM glycine pH 2.5 (Sigma-Aldrich; St. Louis, Missouri, USA) for 5 minutes at room temperature; after incubation, pH was neutralized with 2 M Tris pH 8.0 (Sigma-Aldrich; St. Louis, Missouri, USA), as previously described *[Chow A, Sci Rep 2014]*; to avoid

interference of glycine solution on further analysis, EVs were washed with 3 mL of PBS and pelleted by ultracentrifugation at 100,000 g for 2 hours. HMEC were plated at the same concentration and stimulated with patient derived EVs using the same dose (50.000 EV/cells for EH and 165.000 EV/cells for PA). After 48 hours of treatment, proteins were extracted in RIPA buffer supplemented with 1% Protease Inhibitor Cocktail (Sigma Aldrich, St. Louis, MO, USA). Western blot was performed as described above; 3 ug of total proteins were separated on SDS Page. Blots were incubated with the following primary antibodies: rabbit polyclonal anti-Calreticulin (Abcam #2907, 1:1000), rabbit polyclonal anti-Fibronectin (Abcam #2413, 1:1000), and mouse monoclonal anti-Vinculin (Sigma Aldrich #3574, 1:1000).

2.2.4 Statistical Analysis and Bioinformatics

IBM SPSS Statistics 22 (IBM, New York, USA), Python 3.5 (library, scikit-learn), GraphPad PRISM 7.0a (La Jolla, California, USA), and Cytoscape (National Institute of General Medical Sciences, NIGMS) were used for statistical analyses. Variable distribution was evaluated by Kolmogorov-Smirnov test. Normally distributed variables were expressed as mean ± standard deviation and analyzed by ANOVA with post-hoc Bonferroni test. Non-normally distributed variables were expressed as median and [interquartile range] and analyzed by Kruskal-Wallis test. Categorical variables were expressed as absolute number and (percentage) and analyzed by a chi-square or Fisher tests. Correlations were assessed by Pearson R test and analysis of regression curves. P-values < 0.05 were considered significant.

Supervised learning was used to define a biomolecular signature discriminating patient according to their diagnosis and levels of EV surface antigens. In particular, linear discriminant analysis (LDA) was applied to maximize separations between groups by increasing precision estimate through variance reduction *[James G, Springer Statistics 2014]*. The algorithm uses a set of coefficients to combine EV surface antigen levels in a specific signature and discriminate patients according to their diagnosis. Canonical plot was used to

show discrimination performance.

Protein interactors of the EV surface antigens were retrieved by Cytoscape PESCA plugin, and a global Homo sapiens protein-protein interaction (PPI) network of 1588 nodes and 36984 edges was reconstructed, as previously reported *[Vacchi E Neurol Neuroimmunol Neuroinflamm 2020]*. PPI network was reconstructed considering the first predicted interactors on cell surface of each differentially expressed antigens on EV membrane. The resulting network was analyzed at topological level by Cytoscape Centiscape plugin, to select putative hubs and bottlenecks between the related intracellular signalling targets (taking into account the network size, only nodes with all Betweenness, Bridging, and Centroid values above the average calculated on the corresponding whole network were retained) *[Scardoni G, F1000Res 2014; Scardoni G, F1000Res 2015]*. DAVID database was used to extract enriched Kyoto Encyclopedia of Genes and Genomes (KEGG) pathways and biological processes (Homo sapiens set as background, gene count > 5 and $p<0.001$, corrected by Bonferroni test).

3. RESULTS

In the present study, we delineated for the first time the biomolecular signature of circulating EVs derived from patients affected by PA, taking advantage of a comprehensive evaluation of 37 surface antigens, and supervised machine-learning algorithms. Bioinformatic analysis allowed the identification of potential target of the differentially expressed EV surface antigens, whose functional relevance was explored through an in vitro study.

Serum EVs were isolated by immunocapture from 32 patients with PA, 29 patients with essential hypertension and from 22 normotensive controls. EVs were characterized by western blotting, nanoparticle tracking analysis, transmission electron microscopy, and flow cytometry. Particle concentration was higher and diameter lower in patients with PA compared with controls and the number of particles decreased after unilateral adrenalectomy. Nineteen EV surface antigens were differentially expressed in patients with PA compared with patients with essential hypertension or normotensive controls, including markers of activated platelets, endothelial and immune/ inflammatory cells. The specific EV surface signature discriminated patients with PA from controls, whereas after specific treatment the profile became similar to EH. Stimulation of human endothelial cells with PA-derived EVs resulted in the overexpression of 5 selected genes (*AKT1*, *CALR*, *CSNK2A1*, *FN1*, and *PIK3R1*), previously identified by bioinformatic analysis as targets of differentially expressed EV antigens. Overexpression of *CALR* and *FN1* was confirmed also at protein level.

Our data suggest that EVs may interact with target cells by their surface antigens, thus influencing biomolecular pathways involved in inflammatory response, platelets activation, and modulation of the endocrine system. As surrogate markers of platelets, immune system, and endothelial cells functional state, EVs represent biomarkers of vascular inflammation and endothelial dysfunction in patients with PA and also potential biovectors, contributing to accelerated organ damage by multiple signaling processes.

3.1 *Characteristics of the Study Cohort*

Eighty-three patients were included in the analysis: 22 NT controls, 29 patients with EH, and 32 with PA (20 affected by APA and 12 affected by BiPA). Patients with APA were re-evaluated at 6-12 months after unilateral adrenalectomy (APA post; n=13), whereas patients with BiPA were re-evaluated 6 months of medical treatment with mineralocorticoid receptor antagonists (BiPA post; n=7). Overall, 103 serum samples were analyzed and included in the study. Clinical and biochemical characteristics of patients at baseline are reported in **Table 1**.

No differences were found between NT, EH, and PA with regard to sex, age, weight, BMI, creatinine and lipid profile (p>0.05 for all comparisons). As expected, patients with PA displayed higher systolic and diastolic blood pressure compared with NT controls (154/96 vs. 124/81 mmHg), but not when compared with patients with EH (148/92 mmHg). Similarly, duration of hypertension and antihypertensive treatment (expressed as Defined Daily Dose, DDD, i.e., the assumed average maintenance dose per day for a drug used for its main indication in adults) did not differ between patients with PA and EH. Patients diagnosed with PA vs. EH differed only with regard to potassium, plasma renin activity (PRA), and aldosterone levels; in patients with PA, aldosterone concentration (AC) was higher, and PRA and potassium levels were lower than EH.

After unilateral adrenalectomy, all patients with APA displayed a complete biochemical cure according with PASO criteria *[Williams TA, Lancet Diabetes Endocrinol 2017],* whereas clinical outcome was complete in 38.5% of patients, and partial in 61.5%. Blood pressure levels and DDD decreased compared with the baseline. Potassium level, PRA and AC normalized after surgery (**Table 2**).

Patients with BiPA underwent medical treatment with mineralocorticoid receptor antagonists and displayed a decrease of systolic and diastolic blood pressure and an increase of PRA and potassium levels, consistent with patient compliance to MRA treatment (**Table 3**).

Variable	NT [n=22]	EH [n=29]	PA [n=32]	Overall *P*-value	Pairwise comparisons		
					NT vs EH	NT vs PA	EH vs PA
Sex (Male; %)	9 (40.9)	16 (55.2)	23 (71.9)	0.072	-	-	-
Age (years)	51 ± 9	50 ± 10	48 ± 8	0.382	-	-	-
Duration of HTN (months)	N.A.	8 [4; 19]	7 [2; 13]	0.500	-	-	-
SBP (mmHg)	124 ± 8	148 ± 17	152 ± 16	**<0.001**	**<0.001**	**<0.001**	1.000
DBP (mmHg)	81 ± 4	92 ± 8	95 ± 7	**<0.001**	**0.006**	**<0.001**	0.449
Weight (Kg)	73 ± 9	76 ± 11	78 ± 14	0.312	-	-	-
BMI (Kg/sqm)	25.2 ± 3.2	26.2 ± 2.7	25.7 ± 3.6	0.527	-	-	-
K^+ (mmol/L)	4.2 ± 0.3	4.2 ± 0.3	3.3 ± 0.5	**<0.001**	1.000	**<0.001**	**<0.001**
PRA (ng/mL/h)	N.A.	1.20 [0.80; 1.75]	0.20 [0.10; 0.29]	N.A.	N.A.	N.A.	**<0.001**
AC (ng/dL)	N.A.	10 [7; 14]	30 [25; 44]	N.A.	N.A.	N.A.	**<0.001**
DDD	N.A.	2.00 [0.75; 3.00]	2.25 [1.00; 3.00]	0.383	-	-	-
Dyslipidemia (%)	5 (22.7)	13 (44.8)	11 (34.4)	0.260	-	-	-
Metabolic Snd (%)	1 (4.5)	5 (17.2)	11 (34.4)	**0.025**	0.218	**0.017**	0.155
LVH (%)	0 (0.0)	7 (24.1)	14 (43.8)	**0.001**	**0.015**	**<0.001**	0.177
Total Cholesterol (mg/dL)	183 ± 22	181 ± 39	196 ± 28	0.148	-	-	-
HDL (mg/dL)	46 ± 12	45 ± 12	50 ± 16	0.308	-	-	-
TG (mg/dL)	124 ± 36	128 ± 47	124 ± 55	0.937	-	-	-
Creatinine (mg/dL)	0.9 ± 0.2	1.0 ± 0.1	0.9 ± 0.2	0.385	-	-	-

Table 1. Cohort characteristics *- Clinical and biochemical characteristics of patients with bilateral hyperaldosteronism (BiPA; n=12), compared to BiPA treated with mineralocorticoid antagonists (BiPA post; n=7) and to normotensive controls (NT; n=22) and patients affected by essential hypertension (EH; n=29). HTN, Hypertension; SBP/DBP, Systolic/Diastolic Blood Pressure; PRA, Plasma Renin Activity; AC, Aldosterone Concentration; DDD, Defined Daily Dose; LVH, Left Ventricular Hypertrophy; TG, Triglycerides; N.A., Not Applicable. P-values < 0.05 were considered significant and shown in bold.*

Variable	NT [n=22]	EH [n=29]	APA [n=20]	APA-post [n=13]	Overall *P*-value	Pairwise comparisons					
						NT vs EH	NT vs APA	NT vs APA-p	EH vs APA	EH vs APA-p	APA vs APA-p
Sex (Male; %)	9 (40.9)	16 (55.2)	14 (70.0)	10 (76.9)	0.120	-	-	-	-	-	-
Age (years)	51 ± 9.2	50 ± 10.3	47 ± 7.8	N.A.	0.415	-	-	-	-	-	-
Duration of HTN (months)	N.A.	8 [4;19]	7 [1;11]	N.A.	0.252	-	-	-	-	-	-
SBP (mmHg)	124 ± 8.3	148 ± 16.7	154 ± 18.7	128 ± 7.3	**<0.001**	**<0.001**	**<0.001**	1.000	0.927	**<0.001**	**<0.001**
DBP (mmHg)	81 ± 4.0	92 ± 7.5	96 ± 7.2	80 ± 7.1	**<0.001**	**<0.001**	**<0.001**	1.000	0.605	**<0.001**	**<0.001**
Weight (Kg)	73 ± 8.9	76 ± 10.8	76 ± 14.6	N.A.	0.472	-	-	-	-	-	-
BMI (Kg/sqm)	25.2 ± 3.24	26.2 ± 2.76	25.0 ± 3.58	N.A.	0.338	-	-	-	-	-	-
K^+ (mmol/L)	4.2 ± 0.28	4.2 ± 0.32	3.1 ± 0.44	4.6 ± 0.41	**<0.001**	1.000	**<0.001**	**0.005**	**<0.001**	**0.007**	**<0.001**
PRA (ng/mL/h)	N.A.	1.20 [0.80;1.75]	0.18 [0.10;0.29]	0.80 [0.38;1.20]	**<0.001**	N.A.	N.A.	N.A.	**<0.001**	0.347	**0.011**
AC (ng/dL)	N.A.	10 [7;14]	31 [26;49]	7 [4;10]	**<0.001**	N.A.	N.A.	N.A.	**<0.001**	0.610	**<0.001**
DDD	N.A.	2.00 [0.75;3.00]	3.00 [1.63;3.00]	0.50 [0.00;1.50]	**0.001**	N.A.	N.A.	N.A.	0.539	0.060	**<0.001**
Dyslipidemia (%)	5 (22.7)	13 (44.8)	6 (30.0)	N.A.	0.233	-	-	-	-	-	-
Metabolic Snd (%)	1 (4.5)	5 (17.2)	6 (30.0)	N.A.	**0.039**	0.163	**0.027**	N.A.	0.293	N.A.	N.A.
LVH (%)	0 (0.0)	7 (24.1)	10 (50.0)	N.A.	**0.001**	**0.013**	**<0.001**	N.A.	0.062	N.A.	N.A.
Total Cholesterol (mg/dL)	183 ± 22.2	181 ± 38.8	188 ± 24.0	N.A.	0.681	-	-	-	-	-	-
HDL (mg/dL)	46 ± 11.5	45 ± 11.6	52 ± 18.8	N.A.	0.195	-	-	-	-	-	-
TG (mg/dL)	124 ± 36.0	128 ± 46.7	116 ± 46.6	N.A.	0.649	-	-	-	-	-	-
Creatinine (mg/dL)	0.9 ± 0.15	1.0 ± 0.13	0.9 ± 0.21	N.A.	0.381	-	-	-	-	-	-
Clin Out (n; %) Complete	N.A.	N.A.	N.A.	5 (38.5)							
Clin Out (n; %) Partial	N.A.	N.A.	N.A.	8 (61.5)	-	-	-	-	-	-	-
Clin Out (n; %) Absent	N.A.	N.A.	N.A.	0 (0.0)							
Bioc Out (n; %) Complete	N.A.	N.A.	N.A.	13 (100.0)							
Bioc Out (n; %) Partial	N.A.	N.A.	N.A.	0 (0.0)	-	-	-	-	-	-	-
Bioc Out (n; %) Absent	N.A.	N.A.	N.A.	0 (0.0)							

Table 2. Cohort characteristics: NT vs. EH vs. APA *- Characteristics of patients with an aldosterone producing adenoma (APA; n=20), compared to APA after unilateral adrenalectomy (APA-p; n=13), normotensive controls (NT; n=22), and patients with essential hypertension (EH; n=29). HTN, Hypertension; SBP/DBP, Systolic/Diastolic Blood Pressure; PRA, Plasma Renin Activity; AC, Aldosterone Concentration; DDD, Defined Daily Dose; LVH, Left Ventricular Hypertrophy; TG, Triglycerides; Clin/Bioc outcome according to PASO criteria.*

Variable	NT [n=22]	EH [n=29]	BiPA [n=12]	BiPA-post [n=7]	Overall *P*-value	Pairwise comparisons					
						NT vs EH	NT vs BiPA	NT vs BiPA-p	EH vs BiPA	EH vs BiPA-p	BiPA vs BiPA-p
Sex (Male; %)	9 (40.9)	16 (55.2)	9 (75.0)	5 (71.4)	0.215	-	-	-	-	-	-
Age (years)	51 ± 9.2	50 ± 10.3	49 ± 7.1	N.A.	0.772	-	-	-	-	-	-
Duration of HTN (months)	N.A.	8 [4;19]	11 [2;19]	N.A.	0.785	-	-	-	-	-	-
SBP (mmHg)	124 ± 8.3	148 ± 16.7	147 ± 10.1	131 ± 9.3	**<0.001**	**<0.001**	**<0.001**	1.000	1.000	**0.012**	0.057
DBP (mmHg)	81 ± 4.0	92 ± 7.5	93 ± 5.4	81 ± 8.9	**<0.001**	**<0.001**	**<0.001**	1.000	1.000	**<0.001**	**0.001**
Weight (Kg)	73 ± 8.9	76 ± 10.8	80 ± 14.0	N.A.	0.178	-	-	-	-	-	-
BMI (Kg/sqm)	25.2 ± 3.24	26.2 ± 2.76	26.8 ± 3.56	N.A.	0.295	-	-	-	-	-	-
K^+ (mmol/L)	4.2 ± 0.28	4.2 ± 0.32	3.6 ± 0.50	4.1 ± 0.33	**<0.001**	1.000	**<0.001**	1.000	**<0.001**	1.000	0.066
PRA (ng/mL/h)	N.A.	1.20 [0.80;1.75]	0.20 [0.10;029]	1.12 [0.79;1.60]	**<0.001**	N.A.	N.A.	N.A.	**<0.001**	1.000	**0.009**
AC (ng/dL)	N.A.	10 [7;14]	29 [13;32]	16 [12;17]	**<0.001**	N.A.	N.A.	N.A.	**<0.001**	0.132	1.000
DDD	N.A.	2.00 [0.75;3.00]	1.94 [1.00;2.38]	2.50 [1.25;2.66]	0.573	-	-	-	-	-	-
Dyslipidemia (%)	5 (22.7)	13 (44.8)	5 (41.7)	N.A.	0.246	-	-	-	-	-	-
Metabolic Snd (%)	1 (4.5)	5 (17.2)	5 (41.7)	N.A.	**0.024**	0.163	**0.007**	N.A.	0.098	N.A.	N.A.
LVH (%)	0 (0.0)	7 (24.1)	4 (33.3)	N.A.	**0.022**	**0.013**	**0.004**	N.A.	0.545	N.A.	N.A.
Total Cholesterol (mg/dL)	183 ± 22.2	181 ± 38.8	207 ± 31.4	N.A.	0.059	-	-	-	-	-	-
HDL (mg/dL)	46 ± 11.5	45 ± 11.6	47 ± 11.2	N.A.	0.897	-	-	-	-	-	-
TG (mg/dL)	124 ± 36.0	128 ± 46.7	137 ± 67.2	N.A.	0.766	-	-	-	-	-	-
Creatinine (mg/dL)	0.9 ± 0.15	1.0 ± 0.13	0.9 ± 0.17	N.A.	0.323	-	-	-	-	-	-

Table 3. Cohort characteristics: NT vs. EH vs. BiPA *- Clinical and biochemical characteristics of patients with bilateral hyperaldosteronism (BiPA; n=12), compared to BiPA treated with mineralocorticoid antagonists (BiPA post; n=7) and to normotensive controls (NT; n=22) and patients affected by essential hypertension (EH; n=29). HTN, Hypertension; SBP and DBP, Systolic and Diastolic Blood Pressure; BMI, body mass index; PRA, Plasma Renin Activity; AC, Aldosterone Concentration; DDD, Defined Daily Dose; LVH, Left Ventricular Hypertrophy; TG, Triglycerides; N.A., Not Applicable. P-values < 0.05 were considered significant and shown in bold.*

3.2 EV characterization and Assay Validation

Serum nanoparticles (NPs) were visualized by NTA (**Figure 2A**). NP concentration was higher and particle diameter lower in patients with a diagnosis of PA, compared with both EH and NT controls (2.7- and 5.1-fold increase in particle number, and 1.1- and 1.3-fold decrease in particle diameter, respectively; $p<0.01$; **Table 4** and **Figure 3**). In patient with an APA, the number of NPs declined after unilateral adrenalectomy ($p<0.001$; **Table 5** and **Figure 3**), whereas particle diameter showed an increasing trend.

Patients with BiPA displayed a non-significant decrease of NP concentration and a similar particle diameter, before and after treatment with mineralocorticoid receptor antagonists (**Table 6** and **Figure 3**).

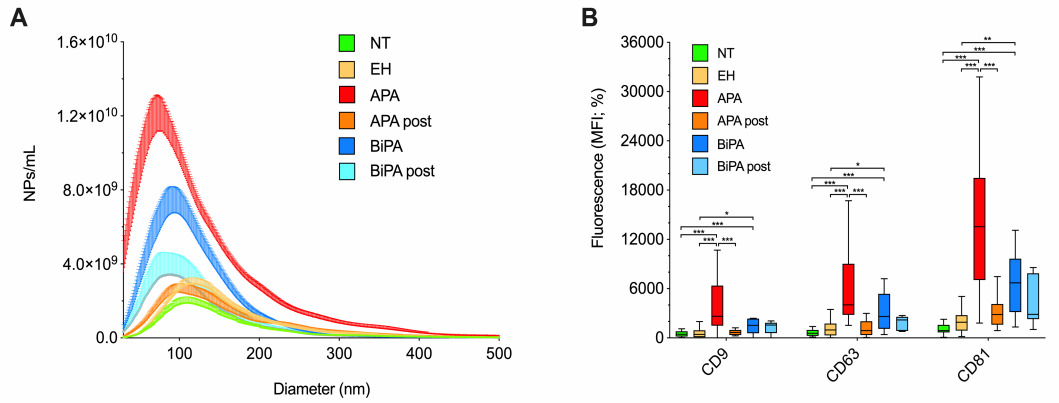

Figure 2 –EV characterization by nanoparticle tracking analysis and flow cytometry - *Data were reported for normotensive subjects (NT; green) vs. patients with essential hypertension (EH; yellow) vs. aldosterone producing adenoma (APA; red) vs. APA after surgery (APA post; orange) vs. bilateral adrenal hyperplasia (BiPA; dark blue) vs. BiPA treated with mineralocorticoid antagonist (BiPA post; light blue). (**A**) Cumulative distribution plot combining nanoparticle (NP) concentration (number of NPs per mL of serum; y axis) and diameter (nm; x axis). (**B**) Median fluorescence intensity (MFI, %) of CD9, CD63, and CD81 by bead-based flow cytometric analysis. Data and statistical analysis: see **Tables 4-6**. Whisker plots show median and interquartile range. *p<0.05; ** p<0.01; *** p<0.001.*

After stratification for particle diameter, patients with PA showed an increase in both small (30-150 nm diameter; 3.2-fold increase) and larger NPs (151-500 nm; 2.1-fold increase) compared with patients affected by EH ($p<0.01$). Patients with an APA displayed a reduction in both small and large particles after surgery (4.8-

fold and 3.2-fold decrease; $p<0.001$), whereas only small NPs were increased in patients with BiPA as compared to EH and NT ($p<0.05$). No differences were found with regard to NP number and diameter between patients with BiPA before and after treatment with mineralocorticoid receptor antagonists (**Tables 4-6**). Taken together these data suggest a prevalent contribution of small NPs to the increase of total NP number observed in patients with PA.

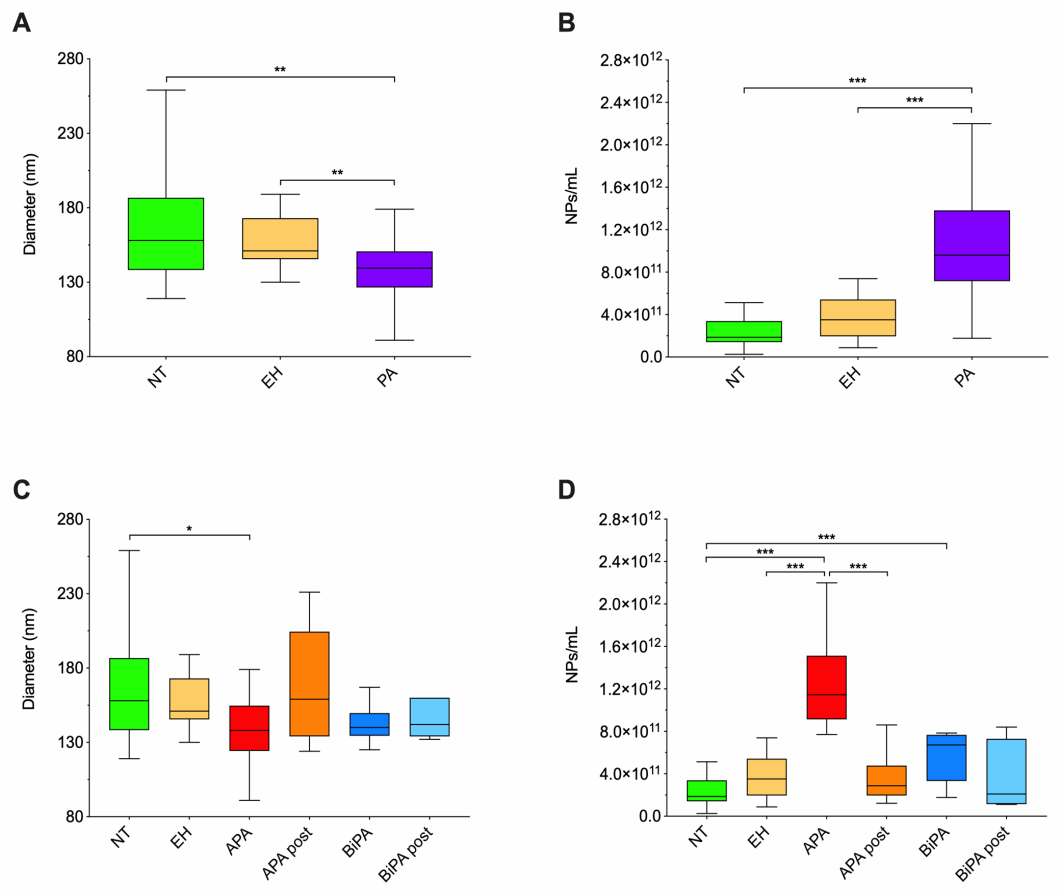

Figure 3. Nanoparticle tracking analysis *- Characterization of extracellular vesicles (EVs) by nanoparticle tracking analysis (NTA) in patients with normotension (NT; green) vs. essential hypertension (EH; yellow) vs. aldosterone producing adenoma (APA; red) vs. APA after surgical intervention (APA post; orange) vs. bilateral hyperaldosteronism (BiPA; dark blue) vs. BiPA treated with mineralocorticoid receptor antagonist (BiPA post; light blue). (**A**, **C**) EV diameter (expressed in nm); (**B**, **D**) Nanoparticle (NP) concentration (expressed as number of NPs per mL of serum). Patients with APA or BiPA are grouped in the category PA (Primary Aldosteronism; purple; panels A and B). Data and statistical analysis: see **Tables 4-6**. Whisker plots show median and interquartile range. *p<0.05; ** p<0.01; *** p<0.001.*

Variable	NT [n=22]	EH [n=29]	PA [n=32]	Overall *P*-value	Pairwise comparisons		
					NT vs EH	NT vs PA	EH vs PA
Diameter (nm)	158 [138;187]	151 [146;173]	140 [127;151]	**0.002**	1.000	**0.005**	**0.008**
NP concentration (n/mL) - [all vesicles]	1.87e11 [1.41e11;3.39e11]	3.51e11 [1.96e11;5.43e11]	9.60e11 [7.16e11;1.38e12]	**<0.001**	0.250	**<0.001**	**<0.001**
NP concentration (n/mL) [30-150 nm]	1.04e11 [4.59e10;2.33e11]	1.92e11 [1.08e11;3.25e11]	6.23e11 [5.00e11;1.02e12]	**<0.001**	0.367	**<0.001**	**<0.001**
NP concentration (n/mL) [151-500 nm]	8.24e10 [5.77e10;1.11e11]	1.40e11 [6.70e10;2.28e11]	2.92e11 [1.96e11;4.14e11]	**<0.001**	0.077	**<0.001**	**0.002**
CD9-CD63-CD81 MFI	7.24 [5.18;12.01]	11.34 [6.88;18.61]	55.96 [34.05;108.45]	**<0.001**	0.281	**<0.001**	**<0.001**

Table 4. EV characterization: NT vs. EH vs. PA *- Extracellular vesicles (EVs) were characterized by nanoparticle tracking analysis (NTA; concentration, expressed as number of nanoparticles [NPs] per mL of serum, and diameter, expressed in nm), and flow cytometric analysis (Median Fluorescence Intensities, MFI, for EV specific markers). Patients with primary aldosteronism (PA; n=32) were compared to normotensive (NT; n=22) and essential hypertensive patients (EH; n=29). P-values < 0.05 were considered significant and shown in bold.*

Variable	NT [n=22]	EH [n=29]	APA [n=20]	APA-post [n=13]	Overall *P*-value	Pairwise comparisons					
						NT vs EH	NT vs APA	NT vs APA-post	EH vs APA	EH vs APA-post	APA vs APA-post
Diameter (nm)	158 [138;187]	151 [146;173]	138 [124;155]	159 [134;205]	**0.018**	1.000	**0.032**	1.000	0.059	1.000	0.121
NP concentration (n/mL) - [all vesicles]	1.87e11 [1.41e11;3.39e11]	3.51e11 [1.96e11;5.43e11]	1.15e12 [9.13e11;1.51e12]	2.87e11 [1.95e11;4.77e11]	**<0.001**	0.341	**<0.001**	1.000	**<0.001**	1.000	**<0.001**
NP concentration (n/mL) [30-150 nm]	1.04e11 [4.59e10;2.33e11]	1.92e11 [1.08e11;3.25e11]	7.49e11 [5.73e11;1.10e12]	1.55e11 [7.54e10;2.95e11]	**<0.001**	0.527	**<0.001**	1.000	**<0.001**	1.000	**<0.001**
NP concentration (n/mL) [151-500 nm]	8.24e10 [5.77e10;1.11e11]	1.40e11 [6.70e10;2.28e11]	3.97e11 [2.83e11;4.60e11]	1.24e11 [7.92e10;1.95e11]	**<0.001**	0.186	**<0.001**	0.891	**<0.001**	1.000	**<0.001**
CD9-CD63-CD81 MFI	7.24 [5.18;12.01]	11.34 [6.88;18.61]	78.85 [48.54;159.20]	16.70 [12.94;25.34]	**<0.001**	0.336	**<0.001**	0.023	**<0.001**	0.942	**0.009**

Table 5. EV characterization: NT vs. EH vs. APA - *Extracellular vesicles (EVs) were characterized by nanoparticle tracking analysis (NTA; concentration, expressed as number of nanoparticles [NPs] per mL of serum, and diameter, expressed in nm), and flow cytometric analysis (Median Fluorescence Intensities, MFI, for EV specific markers. Patients with an aldosterone producing adenoma (APA; n=20) were compared to APA after surgical intervention (APA post; n=13) and to normotensive (NT; n=22) and essential hypertensive patients (EH; n=29). P-values < 0.05 were considered significant and shown in bold.*

Variable	NT [n=22]	EH [n=29]	BiPA [n=12]	BiPA-post [n=7]	Overall *P*-value	Pairwise comparisons					
						NT vs EH	NT vs BiPA	NT vs BiPA-post	EH vs BiPA	EH vs BiPA-post	BiPA vs BiPA-post
Diameter (nm)	158 [138;187]	151 [146;173]	140 [135;150]	142 [134;160]	0.083	-	-	-	-	-	-
NP concentration (n/mL) - [all vesicles]	1.87e11 [1.41e11;3.39e11]	3.51e11 [1.96e11;5.43e11]	6.72e11 [3.33e11;7.67e11]	2.10e11 [1.15e11;7.30e11]	**0.001**	0.168	**<0.001**	1.000	0.125	1.000	0.491
NP concentration (n/mL) [30-150 nm]	1.04e11 [4.59e10;2.33e11]	1.92e11 [1.08e11;3.25e11]	4.74e11 [2.39e11;5.98e11]	1.31e11 [8.24e11;6.05e11]	**0.001**	0.307	**<0.001**	0.759	**0.044**	1.000	0.532
NP concentration (n/mL) [151-500 nm]	8.24e10 [5.77e10;1.11e11]	1.40e11 [6.70e10;2.28e11]	1.55e11 [9.37e10;2.19e11]	7.37e10 [6.27e10;1.67e11]	**0.023**	0.067	0.094	1.000	1.000	0.775	0.582
CD9-CD63-CD81 MFI	7.24 [5.18;12.01]	11.34 [6.88;18.61]	34.07 [23.41;43.33]	25.10 [21.08;31.27]	**<0.001**	0.218	**<0.001**	**0.001**	**0.001**	0.053	1.000

Table 6. EV characterization: NT vs. EH vs. BiPA - *Extracellular vesicles (EVs) were characterized by nanoparticle tracking analysis (NTA; concentration, expressed as number of nanoparticles [NPs] per mL of serum, and diameter, expressed in nm), and flow cytometric analysis (Median Fluorescence Intensities, MFI, for EV specific markers). Patients with bilateral PA (BiPA; n=12) were compared to BiPA treated with mineralocorticoid antagonist (BiPA post; n=7) and to normotensive (NT; n=22) and essential hypertensive patients (EH; n=29). P-values < 0.05 were considered significant and shown in bold.*

The immunocapture assay was validated for its specificity to bind EVs by western blotting and flow cytometry (**Figure 1**). Western blot analysis on representative samples demonstrated the enrichment of TSG101 and Syntenin-1 (as specific markers inside EVs), of CD81 on their membrane, and the depletion of potential contaminants (GRP94 and ApoA1), in EV samples after bead-based immunocapture, as compared to whole serum.

Flow cytometric analysis confirmed the expression of tetraspanins CD9, CD63, and CD81, as specific EV membrane markers. As expected, patients with an APA or with BiPA displayed a significant increase of MFI for CD9-CD63-CD81, compared to controls with EH or NT. Expression of CD9-CD63-CD81 decreased in patients with an APA after adrenalectomy (p<0.05 for all comparisons; **Figure 2B** and **Tables 4-6**). Although NTA cannot discriminate EVs from other particles or lipoproteins in serum, MFI level of tetraspanins at flow cytometry (as a measure of EV concentration) was directly correlated to NP number assessed by NTA (R=0.593; p<0.001; **Figure 4A**). Finally, a direct correlation was found between NP concentration by NTA and systolic / diastolic blood pressure (R= 0.364/0.315; p<0.01), and aldosterone (R=0.473; p<0.001), while an inverse correlation was found with PRA (R= -0.390; p<0.001) and potassium levels (R= -0.598; p<0.001; **Figure 4B-F**).

Bead-based flow cytometric assay used to characterize EV surface antigens was further validated with an alternative protocol and by using high-resolution flow cytometry (HR-FC). Surface profile for representative samples (n=3) was similar after EV enrichment by bead-based immunocapture or ultracentrifugation (median coefficient of variation equal to 0.17; **Figure 5A**). Moreover, levels of CD9, CD63, CD81 and a subset of other EV surface proteins (CD3, CD29, CD25, CD31 and CD45) were highly correlated in samples processed by flow cytometry after bead-based immunocapture *vs.* HR-FC after ultracentrifugation (Pearson's R ranging between 0.660 and 0.919; p<0.05; **Figure 5B-I**). As expected, expression levels for EV antigens decreased after lysis by sonication (**Figure 5L**).

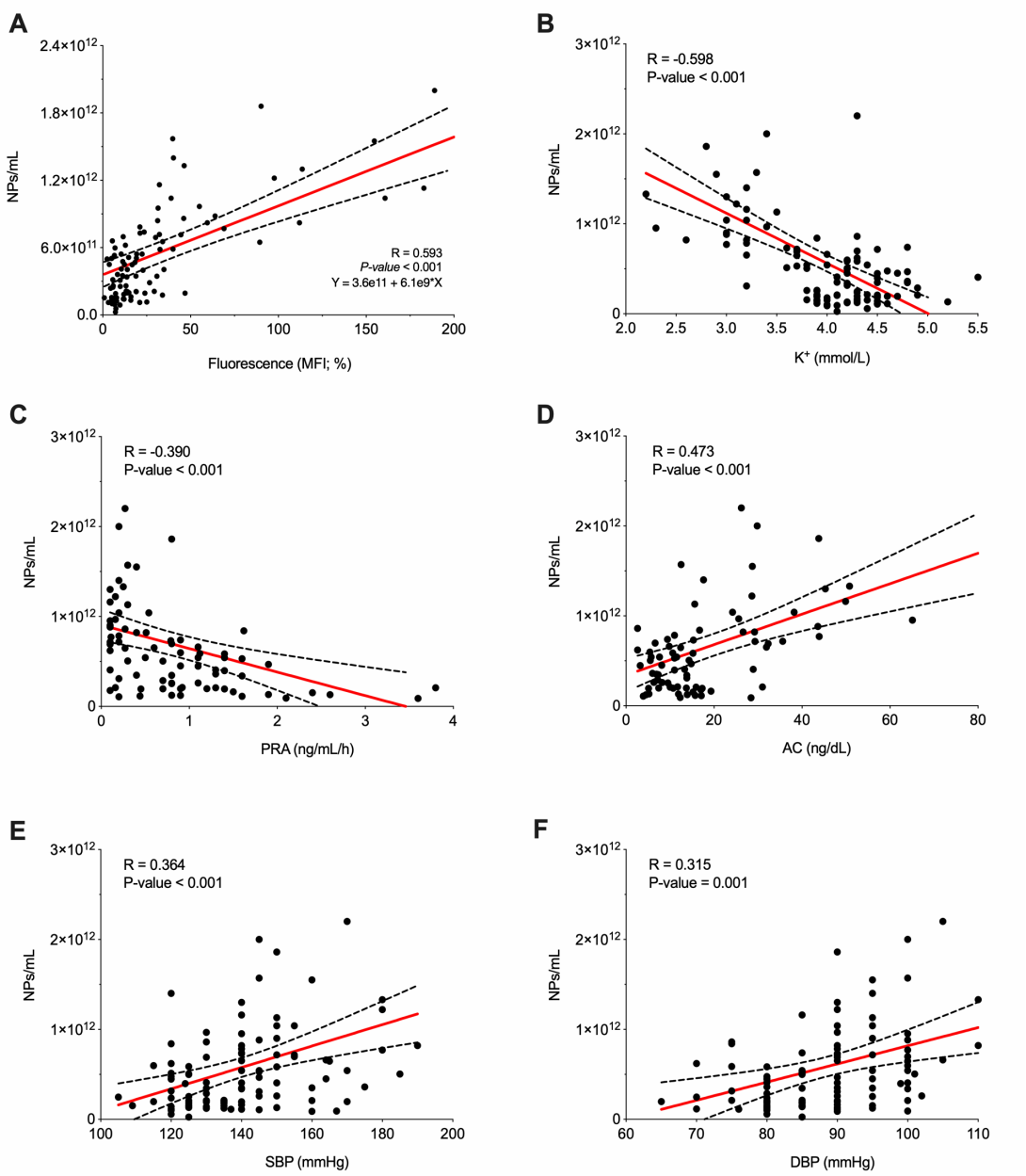

Figure 4. Correlation analysis *- Correlation of nanoparticle (NP) concentration (assessed by nanoparticle tracking analysis and expressed as number of NPs per mL of serum) with:* ***(A)*** *Median fluorescence intensity for CD9, CD63, and CD81 (MFI, %; data from bead-based flow cytometric analysis);* ***(B)*** *Potassium levels (K^+; mmol/L);* ***(C)*** *Plasma renin activity (PRA; ng/mL/h);* ***(D)*** *Aldosterone concentration (AC; ng/dL);* ***(E)*** *Systolic blood pressure (SBP; mmHg);* ***(F)*** *Diastolic blood pressure (DBP; mmHg). The regression line is shown in red together with its 95% confidence interval (dashed lines). Pearson's R coefficient and P-value are reported for each correlation. Differences were considered significant when P-value<0.05. Data and statistical analysis: see* ***Table 11****.*

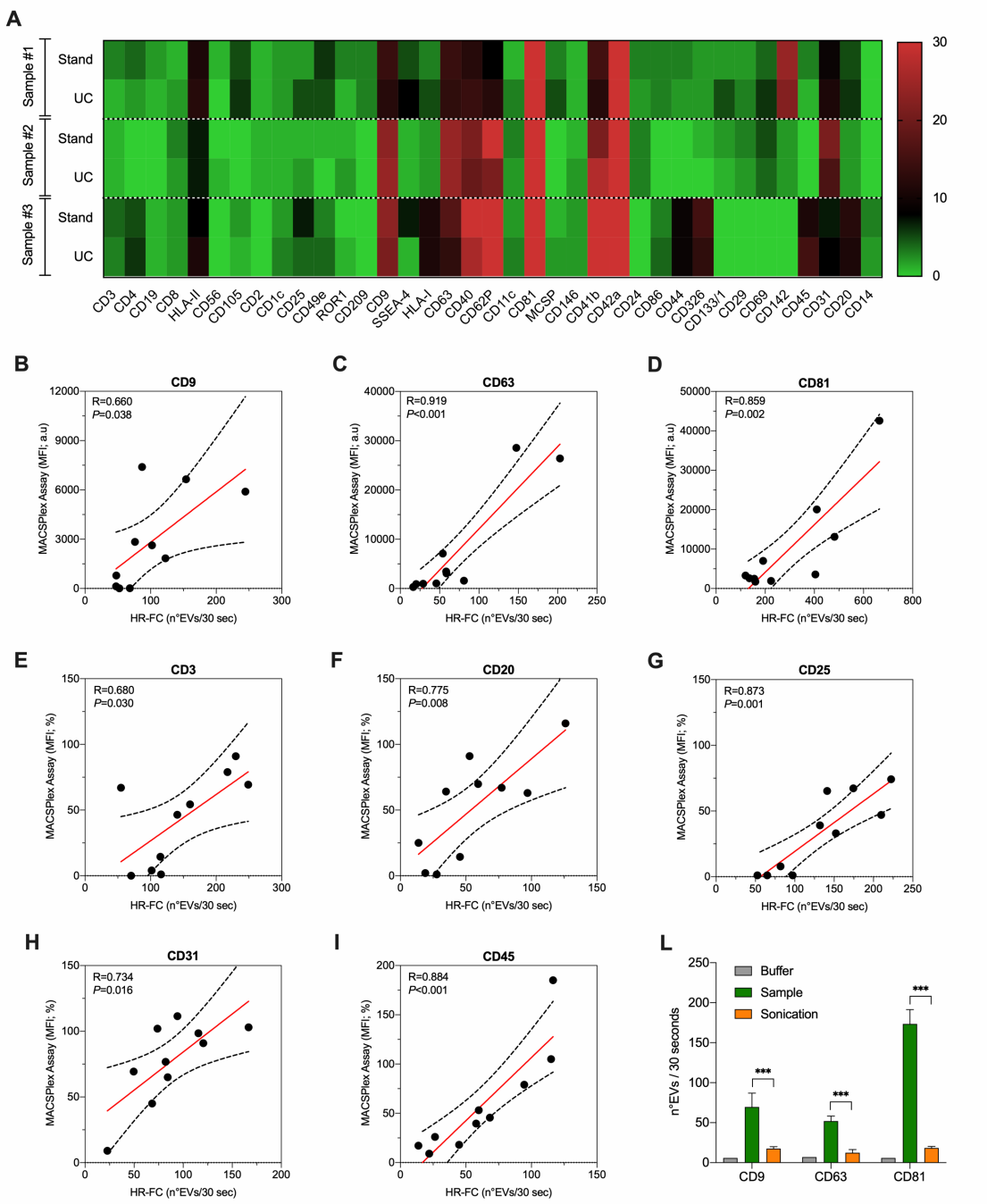

Figure 5. Flow cytometric assay validation - *Bead-based flow cytometric assay used to quantify EV surface antigens was validated by high resolution flow cytometry (HR-FC) and with an alternative protocol. (**A**) Representative samples (n=3) processed with standard protocol (Stand; direct immuno-capture; see methods) compared with pre-isolation by ultracentrifugation (UC) and analyzed by bead-based flow cytometry. (**B-I**) Correlation of EV antigen expression as assessed by HR-FC (x-axis; n°EVs/30 seconds) vs. MACSPlex bead-base flow cytometric assay (y-axis; normalized MFI, %) in 10 subjects (5 PA and 5 EH). (**L**) Lysis control for HR-FC. Samples (n=3) are compared before and after sonication (3 cycle of 30 sec). Buffer is used as referral. *** p<0.001.*

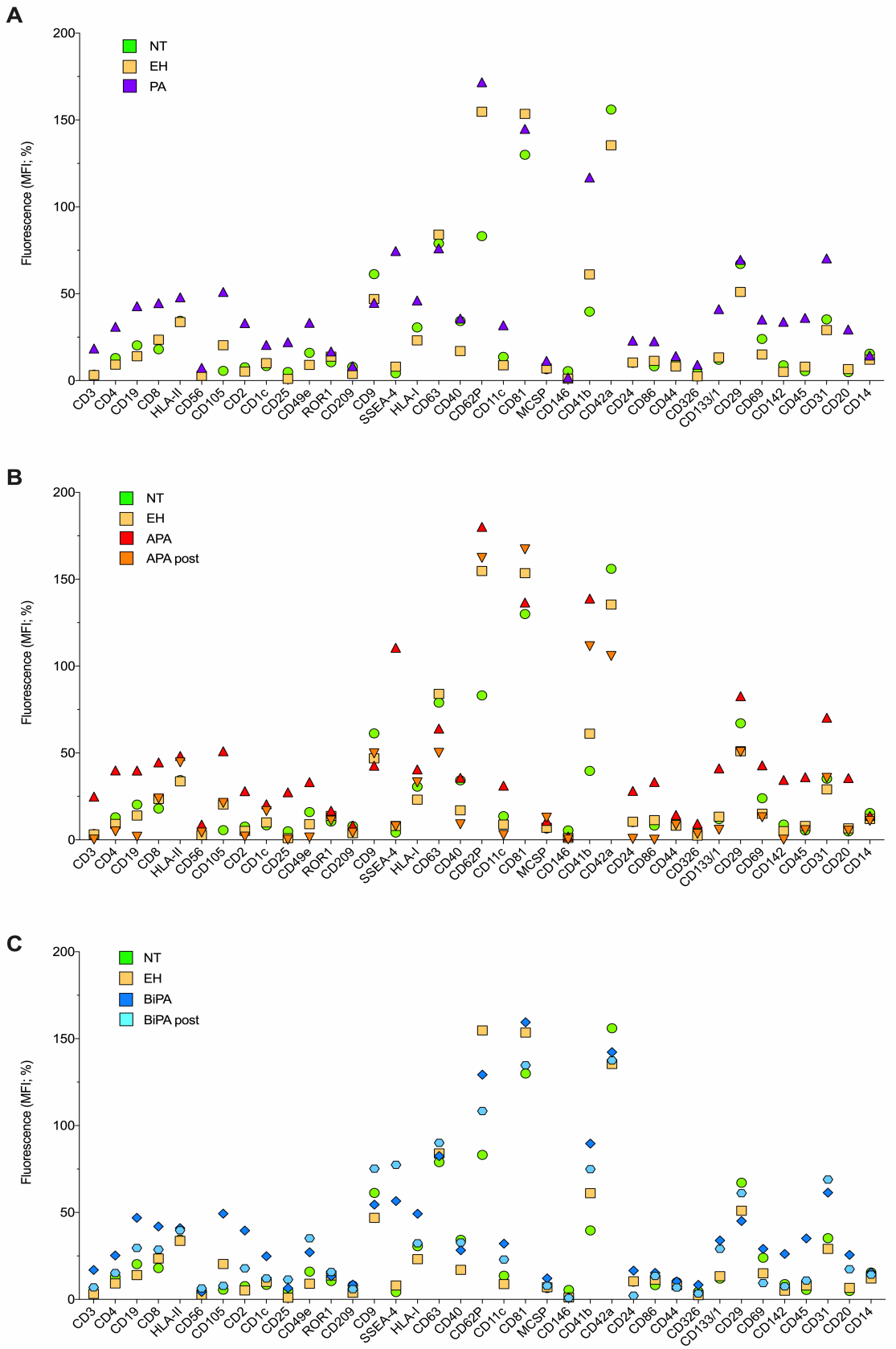
A
B
C
Fluorescence (MFI; %)
200
150
100
50
0
NT
EH
PA
APA
APA post
BiPA
BiPA post
CD3
CD4
CD19
CD8
HLA-II
CD56
CD105
CD2
CD1c
CD25
CD49e
ROR1
CD209
CD9
SSEA-4
HLA-I
CD63
CD40
CD62P
CD11c
CD81
MCSP
CD146
CD41b
CD42a
CD24
CD86
CD44
CD326
CD133/1
CD29
CD69
CD142
CD45
CD31
CD20
CD14

Figure 6. EV surface antigen profiling - *Bead-based flow cytometric analysis of EV surface antigens. Median fluorescence intensities (MFI; %) are reported for all EV antigens after normalization for mean MFI of EV-specific markers (CD9, CD63, CD81). Statistical analysis: see* ***Tables 7-9****. (**A**) Patients with normotension (NT; green) vs. essential hypertension (EH; yellow) vs. primary aldosteronism (PA; purple). (**B**) Patients with an aldosterone producing adenoma (APA; red) were compared to APA after surgery (APA post; orange) and to NT/EH. (**C**) Patients with bilateral PA (BiPA; dark blue) were compared to BiPA treated with MRA (BiPA post; light blue) and to NT/EH.*

3.3 EV surface antigen profile

The profiling of EV surface antigens was performed by flow cytometry after bead-based immuno-capture, according to the protocol shown in **Figure 1**. Immunocaptured EVs from pre-cleared serum were analyzed for the expression of 37 specific surface antigens (**Figure 6**).

Expression levels of each EV surface antigen were normalized by mean MFI of CD9-CD63-CD81 measured in the respective sample, thus providing a specific semi-quantitative analysis for single vesicle.

First, we roughly traced the origin of circulating EVs by grouping surface antigens according to their cellular source. We found that most vesicles originated from platelets or endothelial cells (27% and 15%, respectively; **Figure 7**).

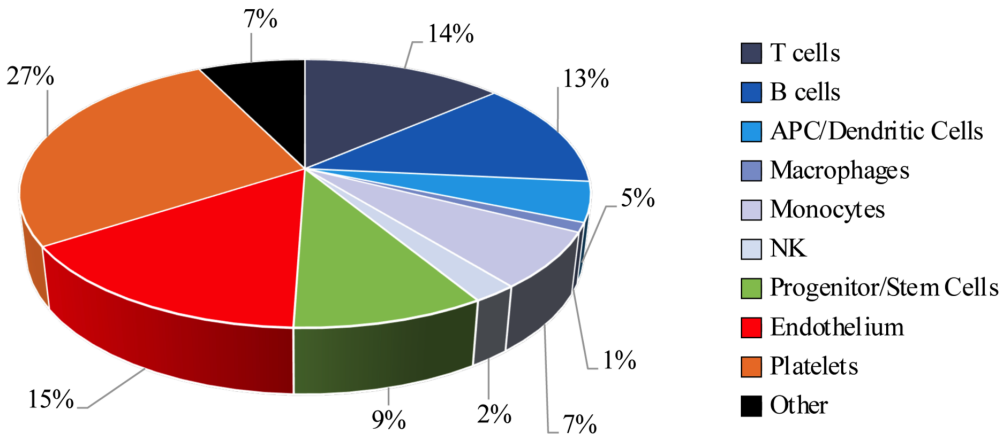

Figure 7. EV origin *- The cell origin of extracellular vesicles (EVs) was determined by bead-based flow cytometric analysis on markers included in a pre-defined panel of antigens (see methods). Markers considered for each cell populations are reported below: T cells (CD2, CD3, CD4, CD8, CD25, CD40, CD45, CD86); B cells (CD11c, CD19, CD20, CD25, CD24, CD40, CD44, CD45); APC/Dendritic cells (CD1c, CD11c, CD209, HLA-II); macrophages (CD11c, CD209); monocytes (CD11c, CD14, CD29, CD49e); NK cells (CD2, CD69); progenitor/stem cells (CD105, CD133/1, SSEA-4); endothelium (CD31, CD62P, CD105, CD146); platelets (CD41b, CD42a, CD62P); other (CD55, CD326, ROR1, HLA-I, MCSP).*

In the overall comparison, 19 EV surface antigens were differentially expressed in patients with PA compared to EH or NT controls (**Tables 7-9**). Eleven antigens showed a differential expression in PA-derived EVs compared with both controls and patients affected by EH: 2 T-cells membrane proteins (CD2, CD3), 1 B-cells membrane proteins (CD20), 2 immune regulatory surface molecules (CD25, CD45), 1 protein involved in endothelial cell function (CD31), 1 platelets glycoproteins (CD41b), 2 coagulation proteins (CD11c, CD142), and 2 stem cells proteins involved in endothelial repair and response to inflammatory insults (SSEA-4 and CD133/1). None of the evaluate antigens showed a differential expression in patients affected by EH compared with normotensive controls (**Table 7**). In patients with an APA, the expression level of these epitopes decreased to the levels observed in patients affected by EH following unilateral adrenalectomy (**Table 8**), thus highlighting a clear cluster in the heat-map of **Figure 8**. CD49e, SSEA-4, and CD41b were also over-expressed in patients with BiPA (**Table 9**). Patients with APA displayed a higher EV concentration compared with BiPA (as assessed by NTA and expression levels of CD9-CD63-CD81 at flow cytometry) and an increased expression of EV surface antigens CD41b and CD42a (**Table 10**).

Correlation analyses were performed to evaluate whether expression levels of EV surface antigens might be related to patients' clinical or biochemical characteristics. As measure of EV number, CD9-CD63-CD81 mean MFI was correlated to aldosterone, PRA, potassium levels, systolic and diastolic blood pressure (R absolute value ranging between 0.318 and 0.519; $p<0.01$; **Table 11**). Several significant correlations were also found between clinical and biochemical parameters and level of expression of each single EV surface antigen (**Table 11**). In the overall population of patients affected by EH or PA, MFI for CD4, CD19, CD41b, CD133/1, CD31, and CD20 were all directly correlated to blood pressure and aldosterone, and inversely correlated to potassium levels (R absolute value ranging between 0.199 and 0.381; $p<0.05$; **Figure 9**).

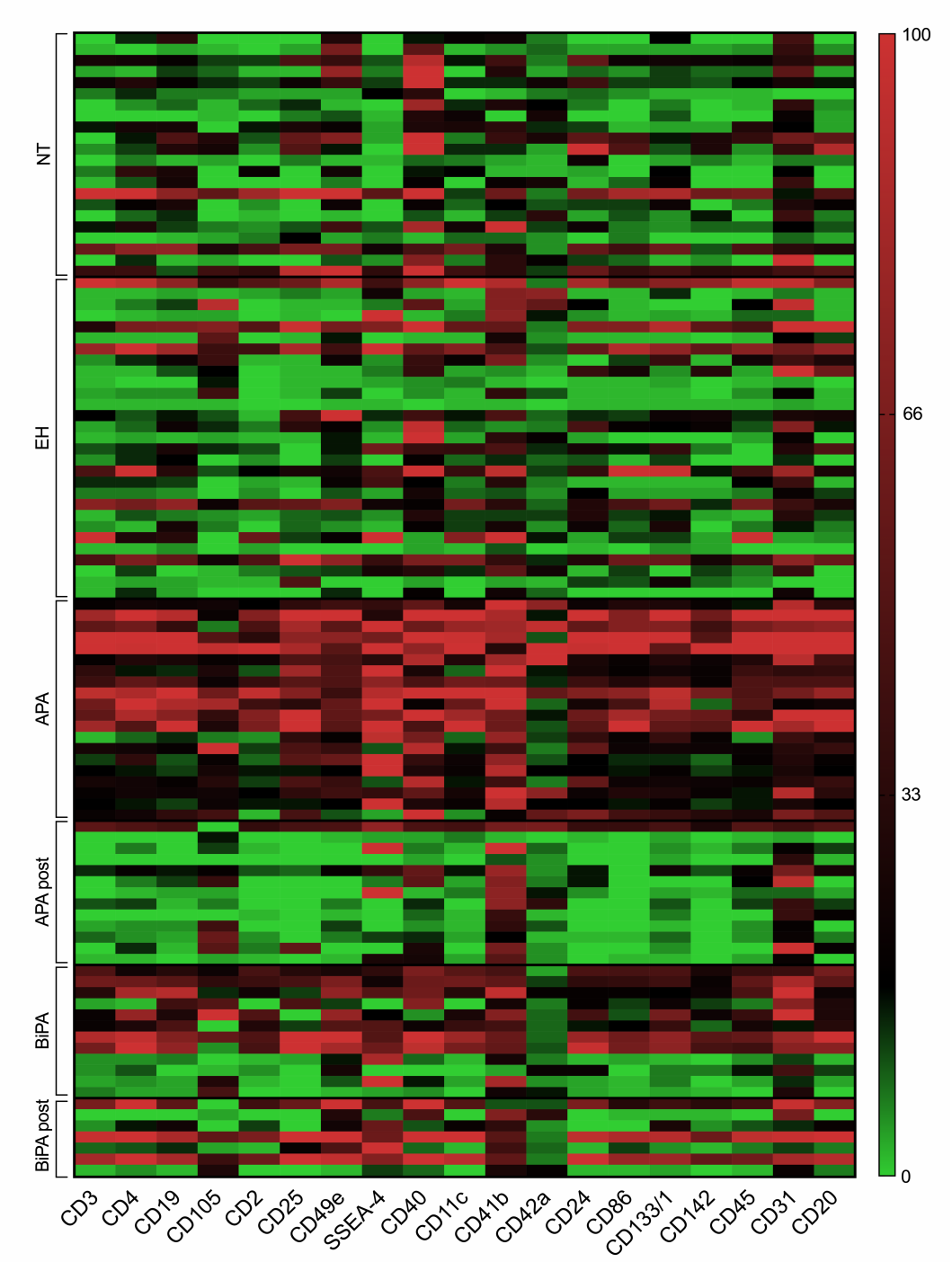

Figure 8. EV surface antigen profile - *Median fluorescence intensity (MFI, expressed as percentage [%], after normalization for mean MFI of CD9, CD63, and CD81; data from bead-based flow cytometric analysis) for differentially expressed EV surface antigens in patients with normotension (NT; n=22) vs. essential hypertension (EH; n=29) vs. aldosterone producing adenoma (APA; n=20) vs. APA after surgery (APA post; n=13) vs. bilateral adrenal hyperplasia (BiPA; n=12) vs. BiPA treated with mineralocorticoid antagonist (BiPA post; n=7). The heat map represents EV surface antigens expression (columns) and patients (row) stratified for diagnosis (red, high fluorescence; green, low fluorescence). Data and statistical analysis: see* ***Tables 7-9****.*

Variable	NT [n=22]	EH [n=29]	PA [n=32]	Overall *P*-value	Pairwise comparisons		
					NT vs EH	NT vs PA	EH vs PA
CD3	3.38 [0.38;14.36]	3.16 [1.00;20.22]	18.46 [6.61;52.07]	**<0.001**	1.000	**0.001**	**0.006**
CD4	13.00 [6.28;27.33]	9.21 [2.00;20.52]	30.97 [11.02;82.58]	**0.003**	1.000	0.073	**0.003**
CD19	20.29 [6.86;31.15]	14.00 [4.50;37.21]	42.81 [14.04;94.61]	**0.023**	1.000	0.150	**0.029**
CD8	18.01 [6.77;43.97]	23.49 [10.00;54.90]	44.60 [21.29;80.05]	0.051	-	-	-
HLA-II	34.42 [18.48;44.00]	33.70 [12.74;86.60]	47.94 [28.13;79.16]	0.168	-	-	-
CD56	3.80 [0.30;11.79]	2.74 [0.00;8.11]	7.37 [3.22;18.30]	0.098	-	-	-
CD105	5.56 [0.00;30.35]	20.40 [2.00;59.49]	51.01 [12.36;93.32]	**0.004**	0.652	**0.004**	0.101
CD2	7.63 [0.74;18.38]	5.18 [1.00;19.10]	33.12 [4.04;68.01]	**0.023**	1.000	**0.048**	**0.046**
CD1c	8.39 [1.04;23.63]	10.07 [1.43;22.70]	20.51 [8.47;47.78]	0.094	-	-	-
CD25	4.92 [0.35;26.02]	1.00 [0.83;21.27]	22.15 [2.44;43.64]	**0.040**	1.000	**0.045**	**0.039**
CD49e	16.02 [4.48;45.98]	9.00 [1.50;15.75]	33.24 [10.59;41.68]	**0.016**	0.528	0.594	**0.012**
ROR1	10.54 [3.06;24.19]	13.76 [2.50;64.21]	16.79 [6.70;35.91]	0.723	-	-	-
CD209	7.94 [1.71;27.53]	3.87 [1.00;17.00]	8.34 [2.16;25.17]	0.631	-	-	-
CD9	61.24 [36.56;73.20]	46.95 [12.45;83.32]	44.73 [20.78;72.59]	0.685	-	-	-
SSEA-4	4.21 [0.39;15.05]	8.00 [2.43;58.00]	74.61 [27.93;139.86]	**<0.001**	0.280	**<0.001**	**0.018**
HLA-I	30.65 [13.15;53.22]	21.13 [8.48;62.00]	46.14 [13.11;60.56]	0.706	-	-	-
CD63	79.00 [64.60;101.94]	84.00 [43.80;112.52]	76.1 [34.65;108.99]	0.822	-	-	-
CD40	34.25 [12.45;70.72]	17.00 [2.62;38.50]	35.74 [13.85;60.04]	**0.037**	0.515	1.000	**0.041**
CD62P	83.11 [37;215.18]	154.74 [104.22;223.64]	171.71 [120.84;217.73]	0.066	-	-	-
CD11c	13.67 [5.50;21.17]	8.84 [2.29;43.04]	31.85 [5.76;84.23]	**0.039**	1.000	**0.044**	**0.035**
CD81	129.99 [117.33;150.46]	153.48 [94.57;234.00]	144.89 [114.65;195.68]	0.238	-	-	-

MCSP	6.56 [0.62;34.03]	7.00 [0.79;28.41]	11.36 [4.32;27.34]	0.341	-	-	-
CD146	5.48 [1.82;13.34]	1.12 [0.56;5.95]	1.76 [0.12;37.22]	0.324	-	-	-
CD41b	39.66 [18.49;61.97]	61.15 [23.76;107.00]	116.92 [64.13;148.09]	**<0.001**	0.318	**<0.001**	**0.009**
CD42a	155.98 [91.23;308.27]	135.43 [90.42;224.46]	224.86 [146.69;311.85]	**0.008**	1.000	0.109	**0.008**
CD24	10.18 [2.92;46.79]	10.46 [1.31;26.42]	22.98 [13.51;51.57]	**0.032**	1.000	0.237	**0.035**
CD86	8.23 [1.97;27.96]	11.38 [1.00;24.02]	22.62 [6.09;68.63]	**0.041**	1.000	**0.046**	0.107
CD44	9.84 [2.07;26.51]	8.18 [1.05;21.36]	14.15 [4.38;30.97]	0.328	-	-	-
CD326	4.44 [0.79;13.99]	2.46 [1.00;16.16]	9.09 [1.42;28.39]	0.332	-	-	-
CD133/1	11.93 [4.08;21.25]	13.36 [2.00;41.59]	41.17 [15.43;71.35]	**0.004**	1.000	**0.012**	**0.014**
CD29	67.10 [34.29;138.76]	51.00 [29.50;97.00]	69.51 [29.97;116.28]	0.560	-	-	-
CD69	23.95 [12.27;46.69]	15.00 [5.20;45.51]	35.15 [14.22;52.10]	0.101	-	-	-
CD142	8.79 [0.98;26.86]	5.00 [1.06;30.34]	33.85 [11.60;73.83]	**0.010**	1.000	**0.036**	**0.026**
CD45	5.47 [0.19;24.54]	8.00 [2.00;35.46]	36.12 [13.96;55.10]	**0.001**	0.847	**0.001**	**0.022**
CD31	35.21 [17.92;44.34]	29.10 [11.99;70.41]	70.37 [31.98;96.02]	**0.004**	1.000	**0.017**	**0.013**
CD20	4.84 [1.94;27.34]	6.62 [0.80;24.67]	29.43 [11.93;65.99]	**0.001**	1.000	**0.009**	**0.003**
CD14	15.50 [8.03;30.04]	12.00 [5.00;20.01]	14.46 [6.66;27.28]	0.506	-	-	-

Table 7. EV surface profiling: NT vs. EH vs. PA - *EV surface profiling by flow cytometric analysis. Median Fluorescence Intensities (MFI; %) are reported for all EV antigens after normalization for mean MFI of EV-specific markers (CD9, CD63, CD81). Patients with primary aldosteronism (PA; n=32) were compared to normotensive controls (NT; n=22) and patients affected by essential hypertension patients (EH; n=29). P-values < 0.05 were considered significant and shown in bold.*

Variable	NT [n=22]	EH [n=29]	APA [n=20]	APA-post [n=13]	Overall *P*-value	Pairwise comparisons					
						NT vs EH	NT vs APA	NT vs APA-post	EH vs APA	EH vs APA-post	APA vs APA-post
CD3	3.38 [0.38;14.36]	3.16 [1.00;20.22]	24.93 [13.80;65.05]	0.15 [0.10;7.68]	**<0.001**	1.000	**0.005**	1.000	**0.028**	0.341	**<0.001**
CD4	13.00 [6.28;27.33]	9.21 [2.00;20.52]	39.98 [16.46;83.40]	4.86 [0.76;12.24]	**<0.001**	1.000	0.063	0.370	**0.002**	1.000	**<0.001**
CD19	20.29 [6.86;31.15]	14.00 [4.50;37.21]	39.87 [15.41;113.95]	1.82 [0.47;10.43]	**0.001**	1.000	0.519	0.054	**0.043**	0.083	**<0.001**
CD105	5.56 [0.00;30.35]	20.40 [2.00;59.49]	51.01 [15.34;92.66]	21.23 [2.73;90.43]	**0.013**	1.000	**0.008**	0.891	0.154	1.000	1.000
CD2	7.63 [0.74;18.38]	5.18 [1.00;19.10]	28.06 [8.23;90.49]	1.88 [0.10;9.29]	**0.003**	1.000	0.136	0.601	0.112	0.445	**0.002**
CD25	4.92 [0.35;26.02]	1.00 [0.83;21.27]	27.37 [10.53;45.98]	0.10 [0.10;2.20]	**0.001**	1.000	0.225	0.117	0.111	0.120	**<0.001**
CD49e	16.02 [4.48;45.98]	9.00 [1.50;15.75]	33.24 [10.99;39.57]	1.33 [0.14;6.25]	**0.001**	1.000	1.000	**0.010**	0.094	0.201	**<0.001**
SSEA-4	4.21 [0.39;15.05]	8.00 [2.43;58.00]	110.54 [41.39;152.95]	7.88 [0.10;74.58]	**<0.001**	0.580	**<0.001**	1.000	**0.025**	1.000	**0.043**
CD40	34.25 [12.45;70.72]	17.00 [2.62;38.50]	35.74 [18.83;68.25]	8.93 [3.35;26.16]	**0.004**	0.242	1.000	**0.034**	0.113	1.000	**0.016**
CD11c	13.67 [5.50;21.17]	8.84 [2.29;43.04]	31.20 [8.98;106.41]	2.85 [0.97;7.29]	**0.002**	1.000	0.149	0.360	0.093	0.314	**0.001**
CD41b	39.66 [18.49;61.97]	61.15 [23.76;107.0]	138.90 [106.07;180.32]	111.45 [49.15;130.10]	**<0.001**	0.698	**<0.001**	0.055	**0.003**	0.968	0.743
CD42a	155.98 [91.23;308.3]	135.43 [90.4;224.5]	256.77 [181.62;1039.4]	105.79 [72.27;201.85]	**<0.001**	1.000	**0.019**	1.000	**0.001**	1.000	**0.002**
CD24	10.18 [2.92;46.79]	10.46 [1.31;26.42]	28.18 [14.24;56.69]	0.61 [0.10;8.72]	**0.001**	1.000	0.466	0.070	0.135	0.133	**<0.001**
CD86	8.23 [1.97;27.96]	11.38 [1.00;24.02]	33.34 [15.09;79.52]	0.10 [0.10;0.92]	**<0.001**	1.000	0.255	**0.012**	0.263	**0.004**	**<0.001**
CD133/1	11.93 [4.08;21.25]	13.36 [2.00;41.59]	41.17 [19.89;76.46]	5.83 [2.57;9.42]	**0.001**	1.000	**0.023**	1.000	**0.018**	1.000	**0.002**
CD142	8.79 [0.98;26.86]	5.00 [1.06;30.34]	34.51 [14.04;85.63]	0.12 [0.10;2.23]	**<0.001**	1.000	0.062	0.296	0.084	0.131	**<0.001**
CD45	5.47 [0.19;24.54]	8.00 [2.00;35.46]	36.12 [16.88;68.38]	5.59 [1.11;15.96]	**0.001**	1.000	**0.002**	1.000	**0.027**	1.000	**0.017**
CD31	35.21 [17.92;44.34]	29.10 [11.99;70.41]	70.37 [34.44;98.60]	35.66 [19.89;56.38]	**0.013**	1.000	**0.028**	1.000	**0.021**	1.000	0.196
CD20	4.84 [1.94;27.34]	6.62 [0.80;24.67]	35.62 [14.98;85.78]	5.31 [0.15;16.70]	**0.002**	1.000	**0.014**	1.000	**0.006**	1.000	**0.012**

Table 8. EV surface profiling: NT vs. EH vs. APA - *EV surface profiling by flow cytometric analysis. Median Fluorescence Intensities (MFI; %) are reported for EV antigens differentially expressed in patients with primary aldosteronism (PA), as compared to normotensive (NT) or essential hypertensive patients (EH; see Table S6), after normalization for mean MFI of EV-specific markers (CD9, CD63, CD81). Patients with an aldosterone producing adenoma (APA; n=20) were compared to APA after surgical intervention (APA post; n=13) and to NT (n=22) and EH patients (n=29). P-values < 0.05 were considered significant and shown in bold.*

Variable	NT [n=22]	EH [n=29]	BiPA [n=12]	BiPA-post [n=7]	Overall *P*-value	Pairwise comparisons					
						NT vs EH	NT vs BiPA	NT vs BiPA-post	EH vs BiPA	EH vs BiPA-post	BiPA vs BiPA-post
CD3	3.38 [0.38;14.36]	3.16 [1.00;20.22]	16.97 [3.90;49.26]	6.92 [1.25;71.45]	0.094	-	-	-	-	-	-
CD4	13.00 [6.28;27.33]	9.21 [2.00;20.52]	25.31 [4.57;78.57]	15.19 [4.40;111.33]	0.326	-	-	-	-	-	-
CD19	20.29 [6.86;31.15]	14.00 [4.50;37.21]	46.95 [5.97;81.50]	29.58 [1.30;107.08]	0.389	-	-	-	-	-	-
CD105	5.56 [0.00;30.35]	20.40 [2.00;59.49]	49.33 [3.68;94.41]	7.77 [0.93;77.60]	0.228	-	-	-	-	-	-
CD2	7.63 [0.74;18.38]	5.18 [1.00;19.10]	39.64 [3.00;65.91]	17.91 [0.75;86.89]	0.546	-	-	-	-	-	-
CD25	4.92 [0.35;26.02]	1.00 [0.83;21.27]	6.48 [0.05;25.39]	11.47 [0.01;77.34]	0.968	-	-	-	-	-	-
CD49e	16.02 [4.48;45.98]	9.00 [1.50;15.75]	27.11 [8.81;54.75]	35.16 [17.05;79.41]	**0.025**	1.000	1.000	0.707	0.146	**0.048**	1.000
SSEA-4	4.21 [0.39;15.05]	8.00 [2.43;58.00]	56.61 [8.95;77.95]	77.46 [14.72;94.23]	**0.004**	0.449	**0.048**	**0.008**	1.000	0.201	1.000
CD40	34.25 [12.45;70.72]	17.00 [2.62;38.50]	28.28 [4.37;48.41]	32.77 [5.47;81.21]	0.211	-	-	-	-	-	-
CD11c	13.67 [5.50;21.17]	8.84 [2.29;43.04]	32.11 [0.81;66.47]	22.90 [0.01;104.43]	0.914	-	-	-	-	-	-
CD41b	39.66 [18.49;61.97]	61.15 [23.76;107.00]	89.67 [47.83;119.54]	74.98 [48.99;96.84]	**0.042**	0.388	**0.046**	0.447	1.000	1.000	1.000
CD42a	155.98 [91.23;308.27]	135.43 [90.42;224.46]	142.22 [113.64;234.15]	137.46 [107.80;288.88]	0.902	-	-	-	-	-	-
CD24	10.18 [2.92;46.79]	10.46 [1.31;26.42]	16.58 [5.78;40.28]	2.16 [0.16;81.25]	0.532	-	-	-	-	-	-
CD86	8.23 [1.97;27.96]	11.38 [1.00;24.02]	15.27 [2.12;47.30]	13.50 [1.77;86.48]	0.683	-	-	-	-	-	-
CD133/1	11.93 [4.08;21.25]	13.36 [2.00;41.59]	33.93 [7.18;66.30]	29.10 [3.55;89.71]	0.324	-	-	-	-	-	-
CD142	8.79 [0.98;26.86]	5.00 [1.06;30.34]	26.18 [5.38;42.35]	7.52 [3.11;93.71]	0.433	-	-	-	-	-	-
CD45	5.47 [0.19;24.54]	8.00 [2.00;35.46]	35.10 [6.23;50.37]	10.87 [2.60;69.12]	0.137	-	-	-	-	-	-
CD31	35.21 [17.92;44.34]	29.10 [11.99;70.41]	61.39 [20.46;89.83]	68.95 [14.52;104.08]	0.276	-	-	-	-	-	-
CD20	4.84 [1.94;27.34]	6.62 [0.80;24.67]	25.63 [5.10;53.93]	17.40 [5.30;80.46]	0.120	-	-	-	-	-	-

Table 9. EV surface profiling: NT vs. EH vs. BiPA - *EV surface profiling by flow cytometric analysis. Median Fluorescence Intensities (MFI; %) are reported for EV antigens differentially expressed in patients with primary aldosteronism (PA), as compared to normotensive (NT) or essential hypertensive patients (EH; see Table S6), after normalization for mean MFI of EV-specific markers (CD9, CD63, CD81). Patients with bilateral PA (BiPA; n=12) were compared to BiPA treated with mineralocorticoid antagonist (BiPA post; n=7) and to NT (n=22) and EH patients (n=29). P-values < 0.05 were considered significant (shown in bold).*

Variable	APA [n=20]	BiPA [n=12]	*P*-value
Diameter (nm)	138 [124;155]	140 [135;150]	0.501
NP concentration (n/mL) - [all vesicles]	1.15e12 [9.13e11;1.51e12]	6.72e11 [3.33e11;7.67e11]	**<0.001**
NP concentration (n/mL) [30-150 nm]	7.49e11 [5.73e11;1.10e12]	4.74e11 [2.39e11;5.98e11]	**0.006**
NP concentration (n/mL) [151-500 nm]	3.97e11 [2.83e11;4.60e11]	1.55e11 [9.37e10;2.19e11]	**<0.001**
CD9-CD63-CD81 MFI	78.85 [48.54;159.20]	34.07 [23.41;43.33]	**<0.001**
CD3	24.93 [13.80;65.05]	16.97 [3.90;49.26]	0.366
CD4	39.98 [16.46;83.40]	25.31 [4.57;78.57]	0.289
CD19	39.87 [15.41;113.95]	46.95 [5.97;81.50]	0.632
CD105	51.01 [15.34;92.66]	49.33 [3.68;94.41]	0.687
CD2	28.06 [8.23;90.49]	39.64 [3.00;65.91]	0.632
CD25	27.37 [10.53;45.98]	6.48 [0.05;25.39]	0.070
CD49e	33.24 [10.99;39.57]	27.11 [8.81;54.75]	0.659
SSEA-4	110.54 [41.39;152.95]	56.61 [8.95;77.95]	0.064
CD40	35.74 [18.83;68.25]	28.28 [4.37;48.41]	0.209
CD11c	31.20 [8.98;106.41]	32.11 [0.81;66.47]	0.195
CD41b	138.90 [106.07;180.32]	89.67 [47.83;119.54]	**0.013**
CD42a	256.77 [181.62;1039.40]	142.22 [113.64;234.15]	**0.002**
CD24	28.18 [14.24;56.69]	16.58 [5.78;40.28]	0.366
CD86	33.34 [15.09;79.52]	15.27 [2.12;47.30]	0.116
CD133/1	41.17 [19.89;76.46]	33.93 [7.18;66.30]	0.408
CD142	34.51 [14.04;85.63]	26.18 [5.38;42.35]	0.326
CD45	36.12 [16.88;68.38]	35.10 [6.23;50.37]	0.346
CD31	70.37 [34.44;98.60]	61.39 [20.46;89.83]	0.477
CD20	35.62 [14.98;85.78]	25.63 [5.10;53.93]	0.289

Table 10. EV characterization: APA vs. BiPA - *Extracellular vesicles (EVs) were characterized by nanoparticle tracking analysis (NTA; concentration, expressed as number of nanoparticles [NPs] per mL of serum, and diameter, expressed in nm), and flow cytometric analysis (median fluorescence intensities, MFI, after normalization for mean MFI of EV-specific markers, CD9, CD63, CD81). Patients with an aldosterone producing adenoma (APA; n=20) were compared to bilateral PA (BiPA; n=12). P-values < 0.05 were considered significant and shown in bold.*

Pearson's test (n=81)	**AC (ng/dL)**		**PRA (ng/mL/h)**		**K^+ (mmol/L)**		**SBP (mmHg)**		**DBP (mmHg)**	
	R	***P*-Value**	**R**	***P*-Value**	**R**	***P*-Value**	**R**	***P*-Value**	**R**	***P*-Value**
NP concentration (n/mL)	**0.473**	**<0.001**	**-0.390**	**<0.001**	**-0.598**	**<0.001**	**0.364**	**<0.001**	**0.315**	**0.001**
CD9-CD63-CD81 MFI	**0.519**	**<0.001**	**-0.318**	**0.004**	**-0.371**	**<0.001**	**0.359**	**<0.001**	**0.348**	**<0.001**
CD3 (%)	0.147	0.192	-0.158	0.159	**-0.273**	**0.005**	**0.268**	**0.006**	0.182	0.066
CD4 (%)	**0.267**	**0.016**	-0.191	0.088	**-0.366**	**<0.001**	**0.201**	**0.042**	**0.210**	**0.033**
CD19 (%)	**0.265**	**0.017**	-0.135	0.229	**-0.363**	**<0.001**	**0.229**	**0.020**	**0.277**	**0.005**
CD105 (%)	-0.010	0.930	-0.057	0.616	-0.059	0.533	0.177	0.074	0.087	0.381
CD2 (%)	**0.234**	**0.035**	-0.151	0.180	**-0.323**	**0.001**	**0.198**	**0.044**	0.050	0.193
CD25 (%)	0.177	0.113	-0.169	0.131	**-0.299**	**0.002**	0.129	0.194	**0.209**	**0.034**
CD49e (%)	0.209	0.061	-0.113	0.316	**-0.206**	**0.037**	0.112	0.260	0.059	0.551
SSEA-4 (%)	**0.303**	**0.006**	**-0.229**	**0.040**	**-0.322**	**0.001**	**0.340**	**<0.001**	0.177	0.074
CD40 (%)	0.217	0.052	-0.056	0.617	**-0.196**	**0.047**	-0.038	0.701	0.001	0.988
CD11c (%)	0.199	0.074	-0.130	0.249	**-0.339**	**<0.001**	**0.238**	**0.015**	**0.263**	**0.007**
CD41b (%)	**0.265**	**0.017**	**-0.290**	**0.009**	**-0.276**	**0.005**	**0.369**	**<0.001**	**0.241**	**0.019**
CD42a (%)	**0.233**	**0.037**	-0.158	0.158	**-0.312**	**0.001**	0.190	0.055	0.173	0.081
CD24 (%)	**0.236**	**0.034**	-0.169	0.132	**-0.348**	**<0.001**	0.139	0.162	**0.219**	**0.026**
CD86 (%)	0.216	0.053	-0.137	0.223	**-0.312**	**0.001**	**0.227**	**0.021**	**0.272**	**0.005**
CD133/1 (%)	**0.269**	**0.015**	-0.128	0.255	**-0.381**	**<0.001**	**0.255**	**0.009**	**0.294**	**0.003**
CD142 (%)	**0.231**	**0.038**	-0.143	0.203	**-0.358**	**<0.001**	0.163	0.100	**0.202**	**0.041**
CD45 (%)	0.192	0.086	-0.172	0.124	**-0.252**	**0.010**	**0.321**	**0.001**	**0.233**	**0.018**
CD31 (%)	**0.282**	**0.011**	-0.158	0.159	**-0.316**	**0.001**	**0.199**	**0.045**	**0.261**	**0.008**
CD20 (%)	**0.257**	**0.021**	-0.102	0.363	**-0.377**	**<0.001**	**0.206**	**0.037**	**0.262**	**0.008**

Table 11. Correlation with clinical and biochemical parameters - *Correlation between clinical and biochemical parameters with EV parameters evaluated by NTA (NP concentration, expressed as number of nanoparticles per mL of serum) and flow cytometric analysis (median fluorescence intensity for CD9-CD63-CD81 and for EV surface antigens differentially expressed in patients with primary aldosteronism, PA). Analysis were performed in patients with a diagnosis of essential hypertension or PA (before and after treatment; n=81). Pearson's R coefficient (left) and P-value (right) are reported for each comparison. AC, Aldosterone Concentration; PRA, Plasma Renin Activity; SBP and DBP, Systolic and Diastolic Blood Pressure. P-values < 0.05 were considered significant and shown in bold.*

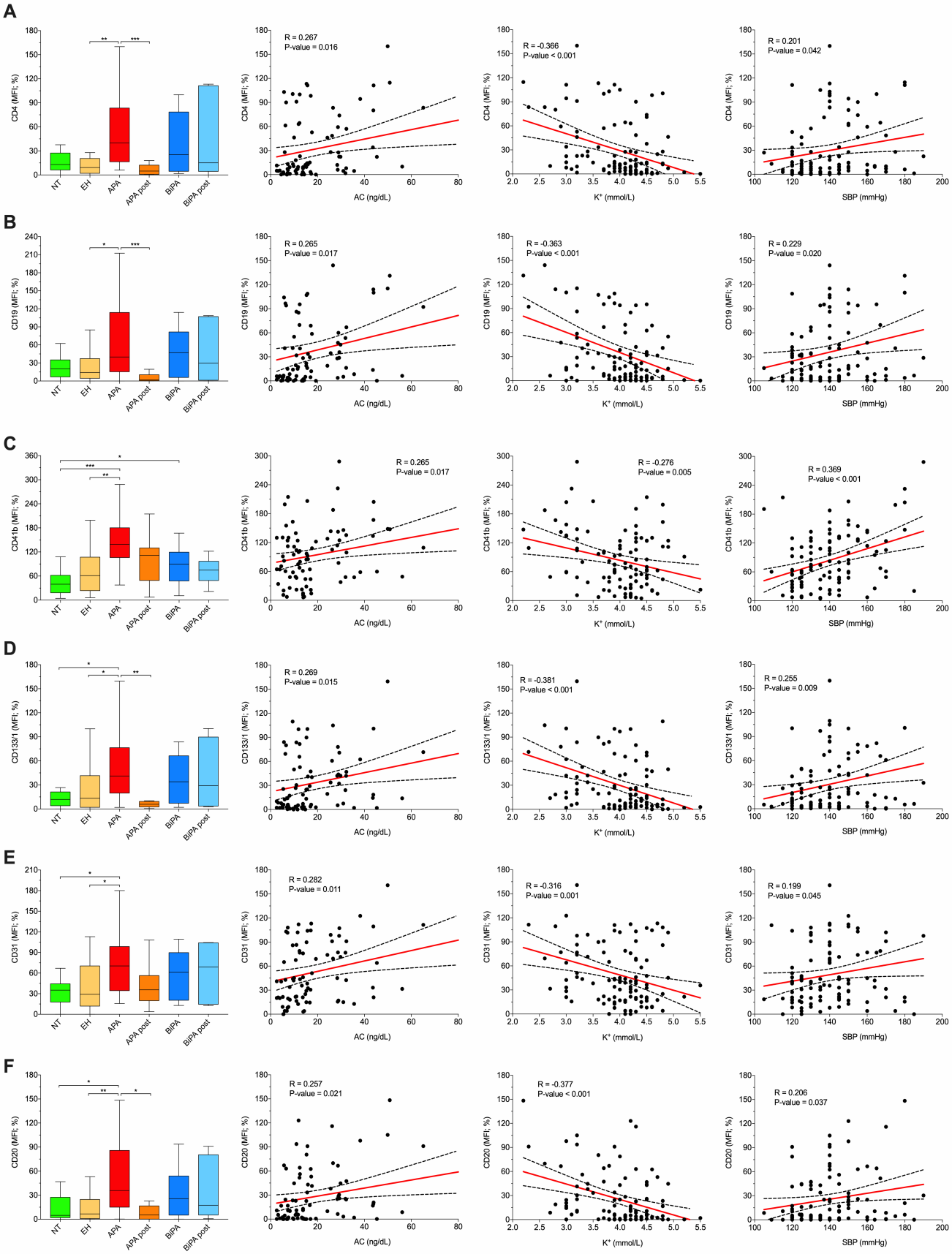
A
CD4 (MFI; %)
NT
EH
APA
APA post
BiPA
BiPA post
R = 0.267
P-value = 0.016
AC (ng/dL)
R = -0.366
P-value < 0.001
K+ (mmol/L)
R = 0.201
P-value = 0.042
SBP (mmHg)
B
CD19 (MFI; %)
R = 0.265
P-value = 0.017
R = -0.363
P-value < 0.001
R = 0.229
P-value = 0.020
C
CD41b (MFI; %)
R = 0.265
P-value = 0.017
R = -0.276
P-value = 0.005
R = 0.369
P-value < 0.001
D
CD133/1 (MFI; %)
R = 0.269
P-value = 0.015
R = -0.381
P-value < 0.001
R = 0.255
P-value = 0.009
E
CD31 (MFI; %)
R = 0.282
P-value = 0.011
R = -0.316
P-value = 0.001
R = 0.199
P-value = 0.045
F
CD20 (MFI; %)
R = 0.257
P-value = 0.021
R = -0.377
P-value < 0.001
R = 0.206
P-value = 0.037

Figure 9. EV surface antigens correlations with clinical/biochemical parameters - *Correlation of EV surface antigens with clinical/biochemical parameters (aldosterone concentration, ng/dL, AC; potassium levels, mmol/L; systolic blood pressure, mmHg, SBP). Median fluorescence intensities (MFI, %; data from bead-based flow cytometric analysis) are reported for indicated EV antigens after normalization for mean MFI of EV-specific markers (CD9, CD63, CD81). Data were reported for normotensive subjects (NT; green) vs. patients with essential hypertension (EH; yellow) vs. aldosterone producing adenoma (APA; red) vs. APA after surgery (APA post; orange) vs. bilateral PA (BiPA; dark blue) vs. BiPA treated with mineralocorticoid antagonist (BiPA post; light blue). (**A**) CD4; (**B**) CD19; (**C**) CD41b; (**D**) CD133/1; (**E**) CD31; (**F**) CD20. Regression line is shown in red, with its 95% confidence interval (dashed lines). Statistical analysis: see **Tables 7-11**. Whisker plots show median and interquartile range. *p<0.05; ** p<0.01; *** p<0.001*

Linear discriminant analysis was used to combine MFI levels of all the differentially expressed EV surface antigens in a specific molecular signature. The canonical plots show patients discrimination according to diagnosis and levels of expression of EV surface antigens (**Figure 10**).

Patients with an APA were clearly discriminated from patients with EH and NT (17 of 20 patients with APA were correctly classified), whereas unilateral adrenalectomy resulted in a significant change of the molecular signature, which became similar to that of patients with EH (**Figure 10A**).

Patients with BiPA were also separated from EH and NT (10 of 12 patients with BiPA correctly classified), whereas after treatment with mineralocorticoid receptor antagonists the EV molecular signature was not significantly different (**Figure 10B**).

Notably, even if singularly none of the evaluated surface epitopes differ significantly between patients affected by EH and normotensive controls, LDA analysis allowed the correct discrimination of the majority of patients with EH from NT controls.

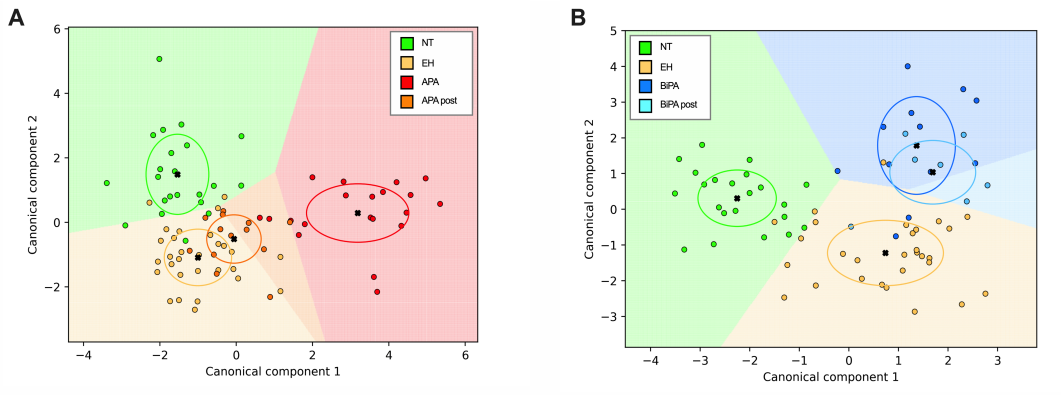

Classification		PREDICTED			
		NT	EH	APA	APA-post
REAL	NT	**19**	3	0	0
	EH	3	**26**	0	0
	APA	0	1	**17**	2
	APA-post	0	2	0	**11**

Classification		PREDICTED			
		NT	EH	BiPA	BiPA-post
REAL	NT	**22**	0	0	0
	EH	1	**27**	1	0
	BiPA	0	2	**10**	0
	BiPA-post	0	1	1	**5**

Figure 10. EV specific signature discriminates patients with PA - *Canonical plots show patient distribution according to their diagnosis and to linear weighted combination of EV surface antigen expression, as assessed by bead-based flow cytometry. Circles indicate patients. Crosses indicate mean values of (canonical-1; canonical-2) for each diagnosis. Ellipses include patients with a linear combination coefficient that falls within the mean +/- SD. If a circle of a defined color (real diagnosis) falls within a graph area of the same color (predicted diagnosis), then the patients is correctly classified according to its diagnosis. (**A**) Discrimination of normotensive subjects (NT; green) vs. patients with essential hypertension (EH; yellow) vs. aldosterone producing adenoma (APA; red) vs. APA after surgery (APA post; orange) (**B**) Discrimination of NT subjects (green) vs. patients with EH (yellow) vs. bilateral adrenal hyperplasia (BiPA; dark blue) vs. BiPA treated with mineralocorticoid antagonist (BiPA post; light blue). Confusion matrix reports real and predicted diagnosis.*

3.4 Bioinformatic Analysis and In Vitro Study

The analysis of protein-protein interaction (PPI) network allowed the identification of protein targets of EVs, as well as molecular functions and biological pathways that could be influenced by EV-surface antigens differentially expressed in patients with PA as compared to EH (**Tables 12-13**).

PPI network was built considering cell surface interactors of differentially expressed antigens on EV membranes. Most relevant intracellular “hubs” or “bottlenecks” were selected among proteins with the greater number of connections or those occupying critical network positions, thus suggesting a pivotal role for the management of the information flow within the related signaling pathway.

Gene name	Protein name	Betweenness	Centroid	Bridging
FN1	Fibronectin	8744	-305	10
PIK3R1	Phosphatidylinositol 3-kinase regulatory subunit alpha	4292	-328	10
ACTB	Actin, cytoplasmic 1	2870	-343	9
ITGB2	Integrin beta-2	2712	-428	21
AKT1	RAC-alpha serine/threonine-protein kinase	2393	-366	9
FLNA	Filamin-A	1928	-373	10
CSNK2A1	Casein kinase II subunit alpha	1464	-378	9
CALR	Calreticulin	1378	-439	15
C1QBP	Complement component 1 Q	1245	-444	27
XRCC6	X-ray repair cross-complementing protein 6	1244	-422	9
EWSR1	RNA-binding protein EWS	1160	-421	10
JUN	Transcription factor AP-1	1022	-397	9
LGALS3BP	Galectin-3-binding protein	1012	-454	23
RANBP9	Importin-9	941	-450	26
SP1	Transcription factor Sp1	888	-435	12
CANX	Calnexin	881	-427	9
INPPL1	Phosphatidylinositol 3,4,5-trisphosphate 5-phosphatase 2	874	-443	17
FASLG	Tumor necrosis factor ligand superfamily member 6	648	-443	18
EZR	Ezrin	643	-432	19
Average Network Value		627	-459	9

Table 12. Network topological analysis - *Intracellular hubs and bottlenecks selected by topological analysis of Protein-Protein Interaction (PPI) network reconstructed considering the first cell surface interactors of each differentially expressed antigen on EV membrane (Primary aldosteronism, PA vs. essential hypertension, EH). Betweenness, Centroid, and Bridging were calculated, and nodes were shown if all indices were above the average derived from the whole network.*

ID Term		Count	*P*-value	Bonferroni
IMMUNE SYSTEM				
hsa04660	T cell receptor signaling pathway	45	7,2E-30	1,5E-27
hsa04650	Natural killer cell mediated cytotoxicity	37	9,3E-18	2,0E-15
hsa04611	Platelet activation	35	5,1E-15	1,1E-12
hsa04670	Leukocyte transendothelial migration	32	3,5E-14	7,4E-12
hsa04662	B cell receptor signaling pathway	33	7,8E-23	1,7E-20
hsa04664	Fc epsilon RI signaling pathway	29	2,1E-18	4,4E-16
hsa04610	Complement and coagulation cascades	22	4,3E-11	9,1E-09
hsa04666	Fc gamma R-mediated phagocytosis	23	3,8E-10	8,0E-08
hsa04630	Jak-STAT signaling pathway	32	2,8E-11	5,9E-09
hsa04620	Toll-like receptor signaling pathway	28	7,3E-12	1,5E-09
hsa04621	NOD-like receptor signaling pathway	17	2,6E-08	5,5E-06
hsa04668	TNF signaling pathway	30	2,1E-13	4,4E-11
SIGNAL TRANSDUCTON				
hsa04151	PI3K-Akt signaling pathway	61	1,5E-16	2,4E-14
hsa04062	Chemokine signaling pathway	46	3,3E-18	7,1E-16
hsa04015	Rap1 signaling pathway	39	3,1E-11	6,6E-09
hsa04014	Ras signaling pathway	44	2,3E-13	4,9E-11
hsa04012	ErbB signaling pathway	32	4,4E-18	9,2E-16
hsa04068	FoxO signaling pathway	27	1,0E-08	2,2E-06
hsa04066	HIF-1 signaling pathway	24	1,0E-09	2,2E-07
hsa04064	NF-kappa B signaling pathway	30	4,2E-16	9,4E-14
hsa04071	Sphingolipid signaling pathway	27	8,6E-10	1,8E-07
hsa04010	MAPK signaling pathway	36	2,6E-07	5,6E-05
hsa04370	VEGF signaling pathway	16	6,2E-07	1,3E-04
ENDOCRINE SYSTEM				
hsa04915	Estrogen signaling pathway	23	1,1E-08	2,3E-06
hsa04917	Prolactin signaling pathway	27	1,2E-15	2,6E-13
hsa04910	Insulin signaling pathway	27	2,0E-08	4,2E-06
hsa04920	Adipocytokine signaling pathway	17	7,6E-07	1,6E-04
hsa04919	Thyroid hormone signaling pathway	23	1,9E-07	4,0E-05
CELLULAR COMMUNITY – EUKARYOTES				
hsa04510	Focal adhesion	53	7,9E-22	1,7E-19
hsa04520	Adherens junction	21	5,9E-10	1,3E-07
SIGNALING MOLECULES AND INTERACTION				
hsa04512	ECM-receptor interaction	19	7,5E-07	1,6E-04
OTHER KEGG CATEGORIES				
hsa04810	Regulation of actin cytoskeleton	36	2,0E-09	4,2E-07
hsa04380	Osteoclast differentiation	40	2,6E-19	5,6E-17
hsa04722	Neurotrophin signaling pathway	36	4,1E-17	8,6E-15
hsa04144	Endocytosis	34	7,5E-07	1,6E-04
hsa04210	Apoptosis	17	1,3E-07	2,7E-05
hsa04960	Aldosterone-regulated sodium reabsorption	15	7,2E-09	1,5E-06

Table 13. Functional evaluation by DAVID database - *KEGG pathways enriched by considering cell surface interactors of each differentially expressed antigen on EV membrane (Primary aldosteronism, PA vs. essential hypertension, EH); enriched pathways were selected considering a gene count > 5 and a P-value <0.001.*

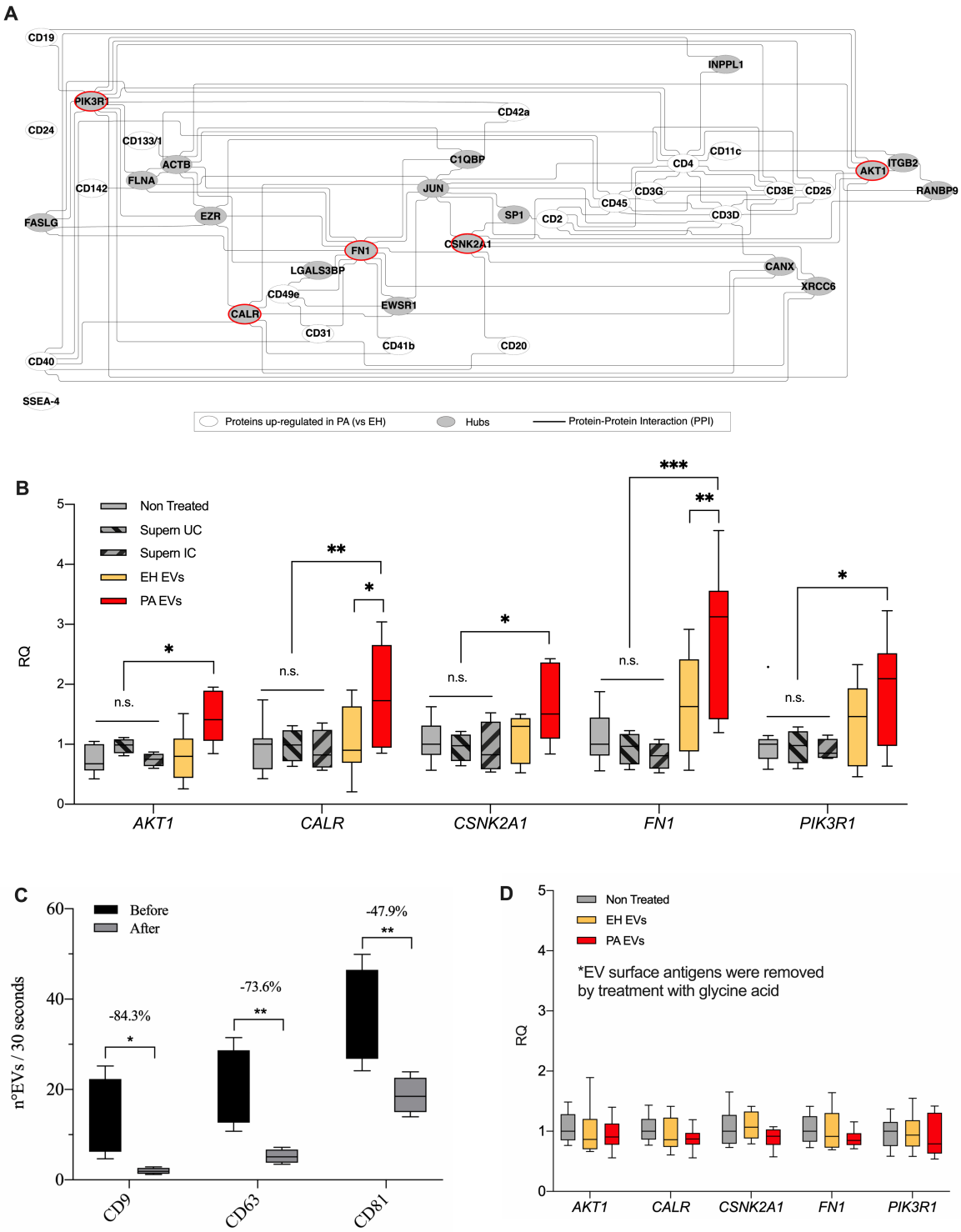

Figure 11. EV-protein interactor network analysis and EV effects on human endothelial cells - *Analysis of protein-protein interaction (PPI) showing intracellular hubs of the network reconstructed by considering cell surface interactors of each differentially expressed EV antigen in patients with primary aldosteronism (PA) vs. essential hypertension (EH). (**A**) PPI network; data and statistical analysis: see **Table 12**. (**B**) EVs effect on expression of selected interactors predicted by analysis of PPI network (highlighted in red in panel A) was evaluated by qRT-PCR. Gene expression of AKT1,*

*CALR, CSNK2A1, FN1, and PIK3R1 was expressed as RQ (relative quantification = $2^{-\Delta\Delta Ct}$), using GAPDH as endogenous reference gene. Human microvascular endothelial cells (HMECs) were treated with PA patient-derived EVs and EH-EVs. Non-treated (NT) cells, cells treated with supernatant after ultracentrifugation (Supern UC) and cells treated with supernatant after bead-based immuno-capture (Supern IC) were used as negative controls. (**C**) EVs were treated with glycine acid to remove EV membrane associated proteins. The graph shows EV quantification at high-resolution flow cytometry (number of EVs/30 seconds; CD9, CD63, and CD81 were used as EV specific markers) before and after glycine treatment. The percentage reduction after treatment was reported for each EV marker. (**D**) Gene expression of AKT1, CALR, CSNK2A1, FN1, and PIK3R1 by qRT-PCR in HMECs stimulated with patient-derived EVs after removal of membrane-associated surface antigens. Reported values are median and interquartile range of triplicates for each condition in 3 independent experiments. *p<0.05; ** p<0.01; *** p<0.001.*

The first 10 hubs for patients with PA were *FN1*, *PIK3R1*, *ACTB*, *ITGB2*, *AKT1*, *FLNA*, *CSNK2A1*, *CALR*, *C1QBP*, and *XRCC6*, (**Figure 11A** and **Table 12**).

EV antigen potential interactors led to the enrichment of pathways related to the immune system and signal transduction, including inflammatory response mediated by T, B, and NK cells, platelets activation, complement and coagulation cascade, cellular adhesion and interaction, and modulation of endocrine system (estrogen, insulin, adipocytes signaling pathways, and aldosterone-regulated sodium reabsorption, among the others; **Figure 12** and **Table 13**).

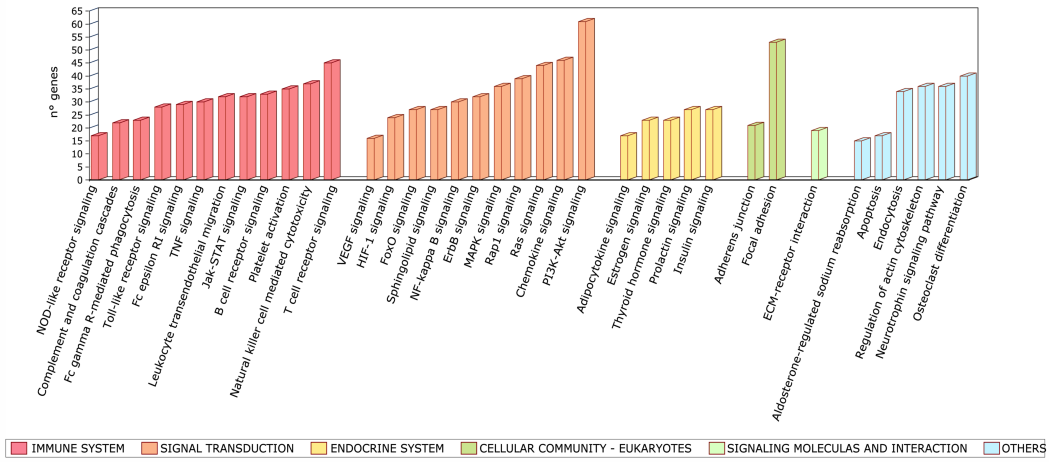

Figure 12. Analysis of enriched pathways after EV treatment - *KEGG intracellular signalling pathways enriched by considering cell surface interactors of each differentially expressed antigen on EV membrane (gene count > 5; p<0.001). Data and statistical analysis: see **Table 13**.*

To explore the effect of patient-derived EVs on potential interactors predicted by PPI network, HMECs were stimulated with PA-EVs or EH-EVs for 24 hours and the expression of mRNA encoding 5 selected targets was examined. EVs for the in vitro study were isolated by ultracentrifugation (see methods). After ultracentrifugation, EV preparation was characterized by nanoparticle tracking analysis, transmission electron microscopy, western blot for specific EV markers and potential contaminants, and flow cytometry for tetraspanins (**Figure 13)**.

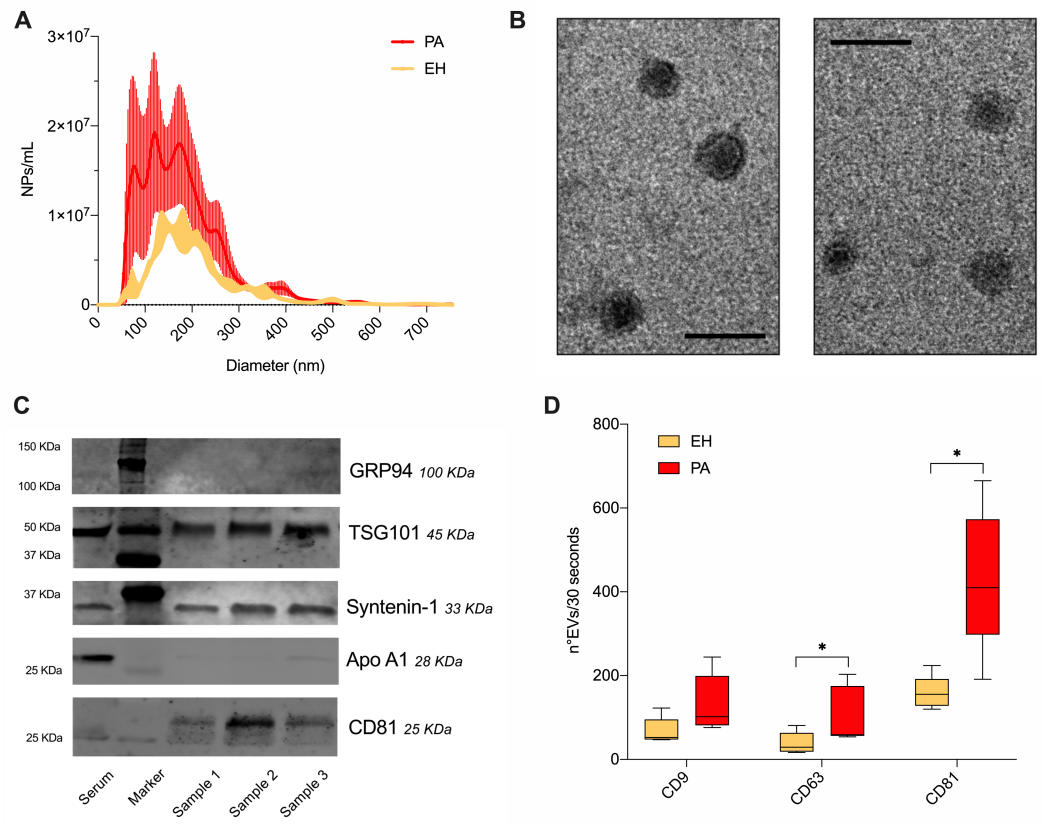

Figure 13. Characterization of EV preparation used for in vitro analysis - *Extracellular vesicles (EVs) used for in vitro analysis were isolated by ultracentrifugation for patients with PA (n=4; red) and EH (n=4; yellow). EV preparation was characterized by NTA, TEM, western blot and flow-cytometry. (**A**) Cumulative distribution plot combining nanoparticle (NP) concentration (number of NPs per mL; y axis) and diameter (nm; x axis). (**B**) Transmission electron microscopy (40.000x magnification; bar 100 nm). Left panel, representative patient with EH; right panel, representative patient with PA. (**C**) Western blot for TSG101, Syntenin-1 and CD81 (specific EV markers) and potential contaminants (GRP94 and ApoA1). (**D**) Expression of CD9, CD63, and CD81 (n°EVs per 30 seconds) by high resolution flow cytometry. *p<0.05.*

Consistently with what we observed characterizing EVs after bead-based immunocapture, after ultracentrifugation the number of NPs from PA patient was higher compared with EH at NTA (2.3-fold increase; $p<0.001$; **Figure 13A**). EVs were also visualized by TEM (**Figure 13B**), which clearly showed the characteristic bilayer phospholipid membrane which distinguishes EVs from lipoproteins or protein aggregates.
Western blot demonstrated the presence of EV specific markers (TSG101, Syntenin-1, and CD81) and the absence of relevant contamination (negligible levels of GRP94 and ApoA1; **Figure 13C**), while the expression of CD9, CD63, and CD81 on EV surface assessed by HR-FC confirmed a significant increase of EV concentration in patients with PA (**Figure 13D**).

Following EV incubation, we demonstrated a significant overexpression of all the selected genes (*AKT1*, *CALR*, *CSNK2A1*, *FN1* and *PIK3R1*) in PA-EVs treated cells compared with non-treated cells, and cells treated with supernatant after either ultracentrifugation, or bead-based immunocapture ($p>0.05$ for all comparisons). Notably, *CALR* and *FN1* displayed a significant overexpression also when PA-EVs treatment was compared to EH-EVs (**Figure 11B**). Finally, the importance of the EV surface antigens on the observed effects on gene expression was confirmed by glycine acid washing to remove EV membrane-associated proteins (see extended methods and **Figure 11C**). After incubation of HMECs with patient EVs lacking their surface proteins, the expression of *AKT1*, *CALR*, *CSNK*, *FN1* and *PIK3R1* did not differ from the non-treated cells (**Figure 11D**).

The over-expression of *CALR* and *FN1* was confirmed also at protein level by western blot on HMECs. After treatment with patient derived EVs, the expression of calreticulin and fibronectin increased in cells treated with PA-EVs compared to both non-treated cells and cells treated with EH-EVs (3.4- and 2.0-fold increase, and 5.0- and 3.3-fold increase, respectively; $p<0.001$; **Figure 14**).

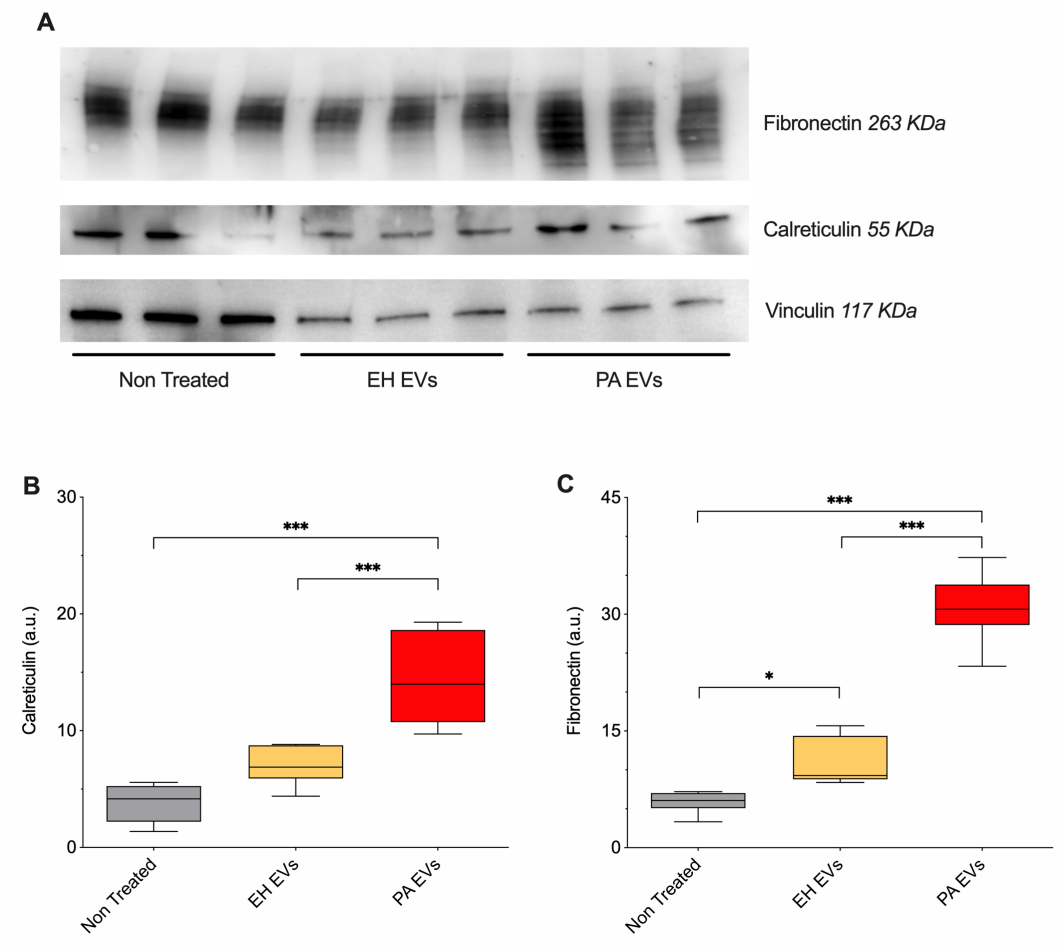

Figure 14. EV effect on protein expression - *EV effect on expression of selected interactors predicted by analysis of PPI network was evaluated by western blot. PA patient-derived EVs and EH-EVs were incubated with human microvascular endothelial cells (HMECs). Non-treated (NT) cells were used as negative controls. (**A**) Representative membranes (the experiment was repeated twice). Protein expression was analyzed after normalization for vinculin, which was used as endogenous control (**B**) Expression of calreticulin (arbitrary unit, a.u.). (**C**) Expression of fibronectin (a.u.). Reported values are median and interquartile range of triplicates for each condition in 2 independent experiments. *p<0.05; *** p<0.001.*

4. DISCUSSION

The role of EVs and their cargo as functional biomarkers or even potential contributors to the development of cardio-metabolic disease is a rapidly expanding area of research. Through the interrogation of surface protein expression and taking advantage of machine-learning algorithms, we demonstrated here that aldosterone excess induces, in patients affected by PA, a distinct circulating EVs biomarker profile, which allows to discriminate them from both normotensive controls and patients affected by EH. Following unilateral adrenalectomy, the expression level of the surface epitopes in patients affected by APA decreased to the level observed in patients affected by EH, suggesting a direct and independent effect of aldosterone. Stimulation of human endothelial cells with EVs derived from patients with PA induced the up-regulation of a number of selected targets, previously identified through bioinformatic network analysis as potential targets of the differentially expressed EV-surface antigens. The effect was specifically dependent on the surface antigens, since it was abolished by removal of EV membrane associated proteins.

Physiologically, the majority of circulating EVs arises from platelets or megakaryocytes, however several pathological conditions may influence EV number and their cellular origin *[Shah R, N Engl J Med 2018]*. An increase in circulating EVs has been extensively reported in both acute and chronic conditions, including myocardial infarction *[Burrello J, J Cell Mol Med 2020]*, diabetes mellitus *[Amabile N, Eur Heart J 2014]*, and atherosclerotic vasculopathy *[Amabile N, Eur Heart J 2014]*. In arterial hypertension, the number of EVs has been correlated with impaired vasoreactivity, arterial stiffness, and blood pressure levels *[Amabile N, Eur Heart J 2014; Preston RA, Hypertension 2003]*, thus reflecting the underlying vascular status.
In our cohort, the total number of small NPs (also referred elsewhere as exosomes *[Yanez-Mo M, J Extracell Vesicles 2015]*) was higher in patients with either APA

or BiPA compared with EH and NT control groups, in agreement with our previous preliminary results *[Burrello J, Hypertension 2019]*.

To perform a systematic characterization of circulating EVs in patients with PA and track their cellular origin, we performed a standardized flow cytometric assay, which allowed the simultaneous evaluation of 37 antigens expressed on EV surface *[Koliha N, J Extracell Vesicles 2016; Wiklander OPB, Front Immunol 2018]*. Five of the 11 antigens differentially expressed between patients affected by PA and both patients affected by EH and NT controls (CD2, CD3, CD20, CD25, and CD45) were represented by T and B cells membrane proteins and immune regulatory surface molecules, suggesting that chronic aldosterone excess elicits the release of extracellular vesicles from immune system cells. This result broadens and further expands our previous findings on a smaller cohort of PA patients, showing an increase in CD45+ (leucocyte derived) EVs in patients with PA compared with normotensive controls *[Burrello J, Hypertension 2019]*.

Beyond its classical role in increasing Na^+ and water reabsorption, aldosterone excess exerts deleterious effects in various organs, including heart, kidney and vasculature *[Mulatero P, Cardiovasc Hematol Agents Med Chem 2006],* which contribute to end-organ damage and cardio-metabolic disease in patients affected by PA *[Monticone S, Lancet Diabetes Endocrinol 2018]*.
In this context, the pioneering contributions of Brilla et al. *[Brilla CG, Circ Res 1990]* showing that aldosterone/salt challenge induces left ventricular fibrosis in rats, opened the way to understanding the several, non-epithelial, aldosterone effects, which comprise the induction of oxidative stress, peri-vascular inflammation and necrosis of the media *[Rocha R, Am J Physiol Heart Circ Physiol 2002]*. Moreover, the fact that cells of the innate and adaptive immune system express the mineralocorticoid receptor (MR) points toward a direct and prominent effect of aldosterone on immune cell activation *[Bene NC, Steroids 2014]*. In mouse macrophages, aldosterone promotes the M1 (classically activated) polarization via its binding to and activation of the MR, while

macrophages from mice lacking the MR in myeloid cells shifted toward the alternative activated M2 phenotype *[Usher MG, J Clin Invest 2010]*.
Similarly, in human monocyte derived macrophages, aldosterone treatment induces trained immunity, a long term pro-inflammatory phenotype with an amplified cytokine response to re-stimulation with different stimuli *[van der Heijden CDCC, Cardiovasc Res 2020]*, which has been suggested to play a role in atherogenesis *[Leentjens J, Circ Res 2018]*.
Other than immune cell system antigens, the specific profile of EVs derived from patients with PA is characterized by the over-representation of stem cell proteins, proteins involved in coagulation, endothelial cell, and platelet function. In particular, compared with EVs derived from patients affected by EH, we observed the over-expression of CD49e (α5 integrin) which, together with β1 integrin, constitutes the fibronectin receptor. Interestingly, in a murine model the conditional inactivation of the mineralocorticoid receptor in the vascular smooth muscle cells, blunted the aldosterone/salt effect on integrin α5 gene expression and arterial stiffness in the carotid artery *[Galmiche G, Hypertension 2014]*.

Additionally, the cytofluorimetric assay results allowed us to obtain, by linear combination of EV surface antigen expression levels, a biomolecular signature able to efficiently discriminate between patients with PA and patients affected by EH or NT controls.
Unilateral adrenalectomy, the treatment of choice for patients affected by APA, significantly affected the expression level of EVs surface proteins, which became similar to the profiling of patients with EH. Considering that surface antigens carried by EVs reflect their cell of origin and its activation state and that it has been showed a role for PA-derived EVs in endothelial cell apoptosis *[Burrello J, Hypertension 2019]*, a possible interpretation of these findings may be related to the reduction of vascular inflammation and improvement of endothelial function after normalization of aldosterone levels by curative adrenalectomy.
On the other side, 6 months of treatment with MRA did not significantly affect EV profiling of patients with BiPA: we speculate that a longer treatment duration

is required to determine a significant effect on endothelial cell function, vascular inflammation, and hence secreted EVs. Consistently, Catena et al. *[Catena C, Hypertension 2007]* observed a decrease in left ventricular mass in PA patients treated with MRA after a mean follow up of 6 years, but not after 12 months.

In our cohort the expression levels of the evaluated surface epitopes did not differ significantly between patients affected by EH and NT controls, while previous studies reported an increase in endothelial and platelet EVs *[Amabile N, Eur Heart J 2014; Preston RA, Hypertension 2003; Helbing T, World J Cardiol 2014]* in patients with hypertension.
It must be acknowledged that in the study by Preston and colleagues the difference was significant only in the subgroup of patients affected by severe hypertension (mean blood pressure of 195/127 mmHg), while we enrolled patients with mild hypertension. Moreover, even if singularly none of the surface epitopes was significantly different, EV signature obtained by LDA discriminated the majority of patients with EH from NT controls. Finally, we should also consider that EH is a multifaced condition which results from the interaction of different factors including vascular tone, sodium and fluid balance and sympathetic tone; this heterogeneity may justify the high dispersion of data, which prevented us to find differences regarding single EV markers in our relatively small cohort of patients affected by EH.

Since EVs mediate autocrine, paracrine, and endocrine signaling by interacting with target cells through their membrane proteins *[Yanez-Mo M, J Extracell Vesicles 2015]*, we performed a bioinformatic network analysis to detect potential interactors of EV surface antigens differentially expressed in patients with PA. Among the predicted hubs, we selected, according to their putative function, the most relevant ones to be confirmed by qRT-PCR. Fibronectin 1 (encoded by *FN1*) is higher in mice treated with aldosterone and is involved in the development of renal fibrosis *[Lai L, Mol Med Rep 2019]*. RAC-alpha serine/threonine-protein kinase, casein kinase II, and calreticulin (encoded by *AKT1*, *CSNK2A1*, and

CALR, respectively) tune renal sodium reabsorption by regulating the epithelial sodium channel ENaC expression and function *[Lee IH, Clin Exp Pharmacol Physiol 2008; Sugahara T, Exp Cell Res 2009; Berman JM, Am J Physiol Renal Physiol 2018]*. Casein kinase II subunit 1 also modulates the activity of mineralocorticoid receptor [*Ruhs S, Sci Rep 2017*] and aldosterone may regulate sodium transport by phosphatidylinositol 3-kinase cascade in renal epithelial cells *[Tong Q, Am J Physiol Renal Physiol 2004]*.

Compared with EH-derived EVs, the stimulation of human endothelial cells with EVs derived from patients with PA induced the overexpression of *CALR* and *FN1*, effect that was abolished by EV surface antigens removal. This finding was confirmed also at protein level. Thus, we can hypothesize a post-transcriptional effect of circulating EVs on endothelial cells, which may be at least in part mediated by the interaction of cells with specific epitopes expressed on the membrane of PA-patients derived EVs.

The analysis of the network also highlights platelets, T- and B- cells activation, complement and coagulation cascade, transendothelial leukocyte migration, adipocytes and insulin signalling pathways, and aldosterone-dependent sodium reabsorption, between the enriched biomolecular pathways. This is consistent with an active role of EVs in determining vascular inflammation and endothelial dysfunction in patients with PA.

The main limitation of our study is that we could not demonstrate if the increase in circulating EVs is a result of PA-associated vascular injury or a direct effect of aldosterone on target cells; the pathological environment of patients with PA, where vessels are exposed to chronically elevated aldosterone levels, inappropriate sodium status and increased shear stress, would not be reproducible in vitro.

5. CONCLUSIONS and PERSPECTIVES

In conclusion, we characterized the surface antigen profile of serum EVs in a large cohort of patients. Circulating EVs, mainly released by platelets, endothelial and inflammatory cells, increased in PA and a specific EV surface signature discriminated these patients. We identified intracellular signalling pathways targeted by differentially expressed EV antigens and demonstrated a functional effect in vitro on human endothelial cells. Our results suggest a role for EVs in the development of endothelial dysfunction, vascular inflammation, and accelerated organ damage in PA.

According with our data, circulating EVs can be considered as active biovectors in patients affected by PA, but the mechanisms by which they are involved in the development of endothelial dysfunction and vascular inflammation remain incompletely understood. Further studies are necessary to investigate the direct effect of aldosterone on the release of EVs by endothelium, inflammatory cells, and platelets, and the molecular mechanism by which in turn may lead to organ damage by interacting with the same endothelial and immune system cells in a vicious detrimental circle.

6. REFERENCES

Amabile N, Cheng S, Renard JM, Larson MG, Ghorbani A, McCabe E, Griffin G, Guerin C, Ho JE, Shaw SY, Cohen KS, Vasan RS, Tedgui A, Boulanger CM, Wang TJ. Association of circulating endothelial microparticles with cardiometabolic risk factors in the Framingham Heart Study. Eur Heart J. 2014;35(42):2972-9. doi: 10.1093/eurheartj/ehu153

Bene NC, Alcaide P, Wortis HH, Jaffe IZ. Mineralocorticoid receptors in immune cells: emerging role in cardiovascular disease. Steroids. 2014;91:38-45. doi: 10.1016/j.steroids.2014.04.005

Berman JM, Mironova E, Stockand JD. Physiological regulation of the epithelial Na+ channel by casein kinase II. Am J Physiol Renal Physiol. 2018;314(3):F367-F372. doi: 10.1152/ajprenal.00469.2017

Bernini G, Galetta F, Franzoni F, Bardini M, Taurino C, Bernardini M, Ghiadoni L, Bernini M, Santoro G, Salvetti A. Arterial stiffness, intima-media thickness and carotid artery fibrosis in patients with primary aldosteronism. J Hypertens. 2008;26(12):2399-405. doi: 10.1097/HJH.0b013e32831286fd

Brilla CG, Pick R, Tan LB, Janicki JS, Weber KT. Remodeling of the rat right and left ventricles in experimental hypertension. Circ Res. 1990;67(6):1355-64. doi: 10.1161/01.res.67.6.1355

Burrello J, Gai C, Tetti M, Lopatina T, Deregibus MC, Veglio F, Mulatero P, Camussi G, Monticone S. Characterization and Gene Expression Analysis of Serum-Derived Extracellular Vesicles in Primary Aldosteronism. Hypertension. 2019;74(2):359-367. doi: 10.1161/HYPERTENSIONAHA.119.12944

Burrello J, Bolis S, Balbi C, Burrello A, Provasi E, Caporali E, Gauthier LG, Peirone A, D'Ascenzo F, Monticone S, Barile L, Vassalli G. An extracellular vesicle epitope profile is associated with acute myocardial infarction. J Cell Mol Med. 2020;24(17):9945-9957. doi: 10.1111/jcmm.15594

Castellani C, Burrello J, Fedrigo M, Burrello A, Bolis S, Di Silvestre D, Tona F, Bottio T, Biemmi V, Toscano G, et al. Circulating extracellular vesicles as non-invasive biomarker of rejection in heart transplant. J Heart Lung Transplant. 2020;39(10):1136-1148. doi: 10.1016/j.healun.2020.06.011

Catena C, Colussi G, Lapenna R, Nadalini E, Chiuch A, Gianfagna P, Sechi LA. Long-term cardiac effects of adrenalectomy or mineralocorticoid antagonists in patients with primary aldosteronism. Hypertension. 2007;50(5):911-8. doi: 10.1161/HYPERTENSIONAHA.107.095448.

Chen ZW, Tsai CH, Pan CT, Chou CH, Liao CW, Hung CS, Wu VC, Lin YH; TAIPAI Study Group. Endothelial Dysfunction in Primary Aldosteronism. Int J Mol Sci. 2019;20(20):5214. doi: 10.3390/ijms20205214

Chow A, Zhou W, Liu L, Fong MY, Champer J, Van Haute D, Chin AR, Ren X, Gugiu BG, Meng Z, Huang W, Ngo V, Kortylewski M, Wang SE. Macrophage immunomodulation by breast cancer-derived exosomes requires Toll-like receptor 2-mediated activation of NF-κB. Sci Rep. 2014;4:5750. doi: 10.1038/srep05750

Farquharson CA, Struthers AD. Aldosterone induces acute endothelial dysfunction in vivo in humans: evidence for an aldosterone-induced vasculopathy. Clin Sci (Lond). 2002;103(4):425-31. doi: 10.1042/cs1030425

Funder JW, Carey RM, Mantero F, Murad MH, Reincke M, Shibata H, Stowasser M, Young WF Jr. The Management of Primary Aldosteronism: Case Detection, Diagnosis, and Treatment: An Endocrine Society Clinical Practice Guideline. J Clin Endocrinol Metab. 2016;101(5):1889-1916. doi: 10.1210/jc.2015-4061

Galmiche G, Pizard A, Gueret A, El Moghrabi S, Ouvrard-Pascaud A, Berger S, Challande P, Jaffe IZ, Labat C, Lacolley P, Jaisser F. Smooth muscle cell mineralocorticoid receptors are mandatory for aldosterone-salt to induce vascular stiffness. Hypertension. 2014;63(3):520-526. doi: 10.1161/HYPERTENSIONAHA.113.01967

Helbing T, Olivier C, Bode C, Moser M, Diehl P. Role of microparticles in endothelial dysfunction and arterial hypertension. World J Cardiol. 2014;6(11):1135-9. doi: 10.4330/wjc.v6.i11.1135.

Ikeda U, Kanbe T, Nakayama I, Kawahara Y, Yokoyama M, Shimada K. Aldosterone inhibits nitric oxide synthesis in rat vascular smooth muscle cells induced by interleukin-1 beta. Eur J Pharmacol. 1995;290(2):69-73. doi: 10.1016/0922-4106(95)90018-7

James G, Witten D, Hastie T, Tibshirani R. Chapter 4.4: Linear discriminant analysis. In: An Introduction to Statistical Learning. Springer texts in Statistics; 2014:138 – 149.

Koliha N, Wiencek Y, Heider U, Jüngst C, Kladt N, Krauthäuser S, Johnston IC, Bosio A, Schauss A, Wild S. A novel multiplex bead-based platform highlights the diversity of extracellular vesicles. J Extracell Vesicles. 2016;5:29975. doi: 10.3402/jev.v5.29975

Lai L, Cheng P, Yan M, Gu Y, Xue J. Aldosterone induces renal fibrosis by promoting HDAC1 expression, deacetylating H3K9 and inhibiting klotho transcription. Mol Med Rep. 2019;19(3):1803-1808. doi: 10.3892/mmr.2018.9781

Lee IH, Campbell CR, Cook DI, Dinudom A. Regulation of epithelial Na+ channels by aldosterone: role of Sgk1. Clin Exp Pharmacol Physiol. 2008;35(2):235-41. doi: 10.1111/j.1440-1681.2007.04844

Leentjens J, Bekkering S, Joosten LAB, Netea MG, Burgner DP, Riksen NP. Trained Innate Immunity as a Novel Mechanism Linking Infection and the

Development of Atherosclerosis. Circ Res. 2018;122(5):664-669. doi: 10.1161/CIRCRESAHA.117.312465

Monticone S, Burrello J, Tizzani D, Bertello C, Viola A, Buffolo F, Gabetti L, Mengozzi G, Williams TA, Rabbia F, Veglio F, Mulatero P. Prevalence and Clinical Manifestations of Primary Aldosteronism Encountered in Primary Care Practice. J Am Coll Cardiol. 2017;69(14):1811-1820. doi: 10.1016/j.jacc.2017.01.052

Monticone S, D'Ascenzo F, Moretti C, Williams TA, Veglio F, Gaita F, Mulatero P. Cardiovascular events and target organ damage in primary aldosteronism compared with essential hypertension: a systematic review and meta-analysis. Lancet Diabetes Endocrinol. 2018;6(1):41-50. doi: 10.1016/S2213-8587(17)30319-4

Mulatero P, Milan A, Williams TA, Veglio F. Mineralocorticoid receptor blockade in the protection of target organ damage. Cardiovasc Hematol Agents Med Chem. 2006;4(1):75-91. doi: 10.2174/187152506775268776

Mulatero P, Monticone S, Deinum J, Amar L, Prejbisz A, Zennaro MC, Beuschlein F, Rossi GP, Nishikawa T, Morganti A, Seccia TM, Lin YH, Fallo F, Widimsky J. Genetics, prevalence, screening and confirmation of primary aldosteronism: a position statement and consensus of the Working Group on Endocrine Hypertension of The European Society of Hypertension. J Hypertens. 2020;38(10):1919-1928. doi: 10.1097/HJH.0000000000002510

Mulatero P, Sechi LA, Williams TA, Lenders JWM, Reincke M, Satoh F, Januszewicz A, Naruse M, Doumas M, Veglio F, Wu VC, Widimsky J. Subtype diagnosis, treatment, complications and outcomes of primary aldosteronism and future direction of research: a position statement and consensus of the Working Group on Endocrine Hypertension of the European Society of Hypertension. J Hypertens. 2020;38(10):1929-1936. doi: 10.1097/HJH.0000000000002520

Preston RA, Jy W, Jimenez JJ, Mauro LM, Horstman LL, Valle M, Aime G, Ahn YS. Effects of severe hypertension on endothelial and platelet microparticles. Hypertension. 2003;41(2):211-7. doi: 10.1161/01.hyp.0000049760.15764.2d

Rizzoni D, Paiardi S, Rodella L, Porteri E, De Ciuceis C, Rezzani R, Boari GE, Zani F, Miclini M, Tiberio GA, Giulini SM, Rosei CA, Bianchi R, Rosei EA. Changes in extracellular matrix in subcutaneous small resistance arteries of patients with primary aldosteronism. J Clin Endocrinol Metab. 2006;91(7):2638-42. doi: 10.1210/jc.2006-0101

Rocha R, Rudolph AE, Frierdich GE, Nachowiak DA, Kekec BK, Blomme EA, McMahon EG, Delyani JA. Aldosterone induces a vascular inflammatory phenotype in the rat heart. Am J Physiol Heart Circ Physiol. 2002;283(5):H1802-10. doi: 10.1152/ajpheart.01096.2001

Ruhs S, Strätz N, Quarch K, Masch A, Schutkowski M, Gekle M, Grossmann C. Modulation of transcriptional mineralocorticoid receptor activity by casein kinase 2. Sci Rep. 2017;7(1):15340. doi: 10.1038/s41598-017-15418-1

Scardoni G, Tosadori G, Faizan M, Spoto F, Fabbri F, Laudanna C. Biological network analysis with CentiScaPe: centralities and experimental dataset integration. F1000Res. 2014;3:139. doi: 10.12688/f1000research.4477.2

Scardoni G, Tosadori G, Pratap S, Spoto F, Laudanna C. Finding the shortest path with PesCa: a tool for network reconstruction. F1000Res. 2015;4:484. doi: 10.12688/f1000research.6769.2

Shah R, Patel T, Freedman JE. Circulating Extracellular Vesicles in Human Disease. N Engl J Med. 2018;379(10):958-966. doi: 10.1056/NEJMra1704286

Sugahara T, Koga T, Ueno-Shuto K, Shuto T, Watanabe E, Maekawa A, Kitamura K, Tomita K, Mizuno A, Sato T, Suico MA, Kai H. Calreticulin positively regulates the expression and function of epithelial sodium channel. Exp Cell Res. 2009;315(19):3294-300. doi: 10.1016/j.yexcr.2009.09.023

Théry C, Witwer KW, Aikawa E, Alcaraz MJ, Anderson JD, Andriantsitohaina R, Antoniou A, Arab T, Archer F, Atkin-Smith GK, et al. Minimal information for studies of extracellular vesicles 2018 (MISEV2018): a position statement of the International Society for Extracellular Vesicles and update of the MISEV2014 guidelines. J Extracell Vesicles 2018;7(1):1535750. doi: 10.1080/20013078.2018.1535750

Tong Q, Booth RE, Worrell RT, Stockand JD. Regulation of Na+ transport by aldosterone: signaling convergence and cross talk between the PI3-K and MAPK1/2 cascades. Am J Physiol Renal Physiol. 2004;286(6):F1232-8. doi: 10.1152/ajprenal.00345.2003

Usher MG, Duan SZ, Ivaschenko CY, Frieler RA, Berger S, Schütz G, Lumeng CN, Mortensen RM. Myeloid mineralocorticoid receptor controls macrophage polarization and cardiovascular hypertrophy and remodeling in mice. J Clin Invest. 2010;120(9):3350-64. doi: 10.1172/JCI41080

Vacchi E, Burrello J, Di Silvestre D, Burrello A, Bolis S, Mauri P, Vassalli G, Cereda CW, Farina C, Barile L, Kaelin-Lang A, Melli G. Immune profiling of plasma-derived extracellular vesicles identifies Parkinson disease. Neurol Neuroimmunol Neuroinflamm. 2020;7(6):e866. doi: 10.1212/NXI.0000000000000866

Van der Heijden CDCC, Smeets EMM, Aarntzen EHJG, Noz MP, Monajemi H, Kersten S, Kaffa C, Hoischen A, Deinum J, Joosten LAB, Netea MG, Riksen NP. Arterial Wall Inflammation and Increased Hematopoietic Activity in Patients With Primary Aldosteronism. J Clin Endocrinol Metab. 2020;105(5):e1967-80. doi: 10.1210/clinem/dgz306

Van der Heijden CDCC, Keating ST, Groh L, Joosten LAB, Netea MG, Riksen NP. Aldosterone induces trained immunity: the role of fatty acid synthesis. Cardiovasc Res. 2020;116(2):317-328. doi: 10.1093/cvr/cvz137

Wiklander OPB, Bostancioglu RB, Welsh JA, Zickler AM, Murke F, Corso G, Felldin U, Hagey DW, Evertsson B, Liang XM, et al. Systematic Methodological Evaluation of a Multiplex Bead-Based Flow Cytometry Assay for Detection of Extracellular Vesicle Surface Signatures. Front Immunol. 2018;9:1326. doi: 10.3389/fimmu.2018.01326

Williams TA, Lenders JWM, Mulatero P, Burrello J, Rottenkolber M, Adolf C, Satoh F, Amar L, Quinkler M, Deinum J, et al; Primary Aldosteronism Surgery Outcome (PASO) investigators. Outcomes after adrenalectomy for unilateral primary aldosteronism: an international consensus on outcome measures and analysis of remission rates in an international cohort. Lancet Diabetes Endocrinol. 2017;5(9):689-99. doi: 10.1016/S2213-8587(17)30135-3

Yáñez-Mó M, Siljander PR, Andreu Z, Zavec AB, Borràs FE, Buzas EI, Buzas K, Casal E, Cappello F, Carvalho J, et al. Biological properties of extracellular vesicles and their physiological functions. J Extracell Vesicles. 2015;4:27066. doi: 10.3402/jev.v4.27066